

ÉCOLE POLYTECHNIQUE FÉDÉRALE DE LAUSANNE
SCHOOL OF LIFE SCIENCES



ÉCOLE POLYTECHNIQUE
FÉDÉRALE DE LAUSANNE

Master project in Bioengineering

**MOVEMENT-RELATED CHARACTERISTICS OF
MIRROR NEURON ACTIVITY IN HUMANS AND
MONKEYS**

Carried out in the Kreiman Laboratory
at Harvard Medical School, Boston
Under the supervision of Antonino Casile, PhD, and Gabriel Kreiman, PhD

Done by

ALICE REGINA MOTSCHI

Under the direction of
Prof. Silvestro Micera
In the laboratory of Translational Neural Engineering (TNE) Lab

EPFL

Lausanne, February 8, 2019

Contents

Acknowledgements	ii
List of Figures	iii
List of Tables	v
Abbreviations	vi
1 Introduction	1
2 Theoretical Background	2
2.1 Mirror neurons	2
2.2 Brain Activity in Specific Frequency Bands	3
2.3 Cortical Layers	4
3 Monkey LFP	5
3.1 Background	5
3.2 Materials and Methods	5
3.2.1 Data Collection	5
3.2.2 Task	5
3.2.3 Data Analysis	5
3.3 Results	6
3.3.1 All Trials	6
3.3.2 Trials by Grip Types	13
3.4 Discussion	16
3.4.1 Time-Frequency Analysis	16
3.4.2 Summed-Up Power	19
3.4.3 Statistically Relevant Distinction of Grip Types with Channel Depth	20
4 Human SEEG	21
4.1 Background	21
4.2 Materials and Methods	21
4.2.1 Data Collection	21
4.2.2 Task	21
4.2.3 Data Analysis	22
4.3 Results	23
4.4 Discussion	23
5 Conclusion	26
References	27

Acknowledgements

First of all, I would like to express my gratitude towards my advisor Antonino Casile who has offered me the project and mentored me throughout its completion.

I also wish to thank Gabriel Kreiman for giving me the opportunity to carry out my Master's thesis in his lab at Boston Children's hospital, Harvard Medical School. The entire group at the Kreiman lab was very welcoming and helpful, which contributed to the amazing atmosphere in the lab and really made me enjoy my stay in Boston. A special thanks goes to Ofer Mazor and Jiarui Wang for their help with hardware issues, to Yuchen Xiao for guiding me through my first experiment with patients, and to Eun-Hyoung Park for her help regarding everything concerning SEEG and the the measurements.

Last but not least I would also like to thank my EPFL supervisor Silvestro Micera to kindly have accepted to oversee this project.

List of Figures

1	Time-frequency analyses of the motor responses from every channel on the two electrodes, GO and NOGO trials. Average of all trials without distinction between the grip types. The plots on the top left of each panel correspond to the most superficial channel, plots on the bottom right to the deepest channel. NOGO trials were aligned with CueOn and GO trials were aligned with ObjTouch (time $t = 0$ s). The vertical black lines correspond to the average time of the occurrence of the events in the order: CueOn , GoSignal , ArmLift , ObjTouch , ObjRelease , RewardUp , the black shade being the standard deviation. For NOGO trials, the events from ArmLift to ObjRelease are virtual.	7
2	Average power recorded by the third most superficial channel of electrode 2 in the frequency band 15 Hz to 25 Hz with respect to the baseline for motor and visual responses. GO trials are aligned at ObjTouch (blue, time line: lower x-axis), NOGO trials are aligned at CueOn (red, time line: upper x-axis). The vertical lines from left are: (dashed) visual CueOn , (solid) motor CueOn , (dotted) motor and visual ObjTouch , (solid) motor ObjTouch , (dashed) visual ObjTouch , all mean values and with respect to the GO trials.	8
3	Average power recorded by the third most superficial channel of electrode 2 in the frequency band 40 Hz to 60 Hz with respect to the baseline for motor and visual responses. GO trials are aligned at ObjTouch (blue, time line: lower x-axis), NOGO trials are aligned at CueOn (red, time line: upper x-axis). The vertical lines from left are: (dashed) visual CueOn , (solid) motor CueOn , (dotted) motor and visual ObjTouch , (solid) motor ObjTouch , (dashed) visual ObjTouch , all mean values and with respect to the GO trials.	9
4	Time-frequency analyses of the visual responses from every channel on the two electrodes, GO and NOGO trials. Average of all trials without distinction between the grip types. The plots on the top left of each panel correspond to the most superficial channel, plots on the bottom right to the deepest channel. NOGO trials were aligned with CueOn (time $t = 0$ s) and GO trials were aligned with ArmLift (time $t = 0$ s). The vertical black lines correspond to the average time of the occurrence of the events in the order: CueOn , GoSignal , ArmLift , ObjTouch , ObjRelease , RewardUp , the black shade being the standard deviation. For NOGO trials, the events from ArmLift to ObjRelease are virtual.	10
5	Summed up power of the motor responses in time and frequency ranges of interest. The bold lines correspond to the linear regression of the summed up power with electrode depth (see legend for Pearson correlation coefficient). If there is no line, the correlation was not significant. 1 is the most superficial, 16 the deepest channel.	11
6	Summed up power of the visual responses in time and frequency ranges of interest. The bold lines correspond to the linear regression of the summed up power with electrode depth (see legend for Pearson correlation coefficient). If there is no line, the correlation was not significant. 1 is the most superficial, 16 the deepest channel.	12
7	Time-frequency analyses of both the motor and visual responses from the third most superficial channel on electrode 2, GO and NOGO trials and the three grip types. Average of all trials. NOGO trials for both tasks were aligned with CueOn , motor GO trials were aligned with ObjTouch and visual GO trials were aligned with ArmLift (time $t = 0$ s). The vertical black lines correspond to the average time of the occurrence of the events in the order: CueOn , SignalOn , ArmLift , ObjTouch , ObjRelease , RewardUp , the black shade being the standard deviation. For NOGO trials, the events from ArmLift to ObjRelease are virtual.	14

8 Average power recorded by the third most superficial channel of electrode 2 in the frequency band 40 Hz to 60 Hz with respect to the baseline for motor (left panel) and visual (right panel) responses. GO trials are aligned at **ObjTouch** (blue, time line: lower x-axis), **NOGO** trials are aligned at **CueOn** (red, time line: upper x-axis). The vertical lines in both panels correspond to (left) **CueOn**, (middle) **ObjTouch**, (right) **ObjRelease**, all mean values and with respect to the GO trials. 14

9 Pearson correlation coefficient for motor and visual responses between channel depth and grip type distinction score for different time and frequency ranges. A positive correlation means that the deeper channels can better distinguish between the grip types, a negative correlation that the more superficial channels are better in doing so. An asterisk marks statistically significant correlations ($\alpha = 0.05$). 15

10 Picture of the board used for human experiments. (1) corresponds to prehension grip, (2) to precision grip, and (3) to power grip. (4) is the resting hand plate. For dimensions see text. 21

11 Time-frequency analyses of the human visual responses from the six electrodes of interest, GO and NOGO trials and the three grip types. Average of all trials. The plot on the top left (11a) corresponds to the most superficial channel, the plot on the bottom right (11f) to the deepest channel. NOGO trials were aligned with **CueOn** and GO trials were aligned with **ObjTouch** (time $t = 0$ s). The vertical black lines correspond to the average time of the occurrence of the events in the order: **CueOn**, **GoSignal**, **ObjTouch**, **ObjRelease**, **HandBack**, the black shade being the standard deviation. For NOGO trials, only **CueOn** is plotted. 24

List of Tables

1	Number of trials in the motor task that remained after removal of artifacts, depending on the channel.	6
2	Number of trials in the visual task that remained after removal of artifacts, depending on the channel.	6
3	Maximum distinction score for motor responses, GO trials.	16
4	Maximum distinction score for motor responses, NOGO trials.	16
5	Maximum distinction score for visual responses, GO trials.	16
6	Maximum distinction score for visual responses, NOGO trials.	16
7	Numbers of trials in the SEEG experiment with a human patient (only visual condition) that remained after removal of artifacts, depending on the channel. .	22
8	Student's t-significant differences between grip type combinations ($\alpha = 0.05$). Preh: Prehension. Prec: Precison. Pow: Power.	25
9	Student's t-significant differences between conditions ($\alpha = 0.05$).	25

Abbreviations

CueOn	Moment at which the LED next to an object was turned on in order to cue the object that, in the case of GO trials, needed to be touched
GoSignal	Moment at which the sound stopped playing; in the case of GO trials, the participant or experimenter was allowed to start moving their hand
ArmLift	Moment at which the participant or experimenter no longer touches the hand resting plate
ObjTouch	Moment at which the object was touched by the participant or the experimenter
ObjRelease	Moment at which the object was no longer touched by the participant or the experimenter
RewardUp	Moment at which the monkey was given a reward at the end of the trial
HandBack	Moment at which the (human) participant or the experimenter put their hand back on the hand resting plate
ECOG	Electrocorticography
EEG	Electroencephalography
fMRI	Functional magnetic resonance
LFP	Local field potential
MEG	Magnetoencephalography imaging
SEEG	Stereoelectroencephalography

Movement-Related Characteristics of Mirror Neuron Activity in Humans and Monkeys

Abstract. Mirror neurons may play an important role in communication. Nevertheless, this topic hasn't been studied rigorously in humans using intracranial techniques.

In this project, power modulations of LFPs (local field potentials) recorded from monkey motor area F5 were analyzed with regard to characteristic patterns during a grasping task. These characteristics were compared to the visual responses recorded during observation of the same task. Three important frequency ranges could be identified: (1) 40 Hz to 60 Hz: power increase related to movement. (2) 15 Hz to 25 Hz: power decrease related to movement preparation, execution, and suppression. (3) 0.1 Hz to 8 Hz: power increase related to movement and other processes. All of these patterns were observed in the visual responses as well. However, the different grip types could not always be distinguished with statistical significance.

In order to ascertain if the monkey serves as a good model for humans, the same experiment was repeated with an epilepsy patient using SEEG (stereoelectroencephalography). Some characteristics were similar in human and monkey responses, but there were also differences. The main limitation here is the fact that the patient was recovering from a brain surgery and therefore was not in the best condition to perform the experiment. Nevertheless, a first impression of the comparison between human and monkey mirror systems could be made.

1 Introduction

This Master's thesis is part of a bigger project carried out by Dr. Antonino Casile¹ and Dr. Gabriel Kreiman². Its aim is to give insight into the neural mechanisms that allow us to perceive and understand the actions of others, which is crucial in order to engage in social interactions.

Observing others' actions evokes some activity in the motor areas, but it is still under

¹Center for Translational Neurophysiology, Istituto Italiano di Tecnologia, Ferrara, Italy

²Department of Ophthalmology, Boston Children's Hospital, Harvard Medical School, Boston, USA

debate which information is encoded [1]. Presumably, many different processes take place at the same time in different regions, therefore, in order to dissolve the mechanisms, high resolution recordings are required. However, when conducting experiments with humans, often non-invasive techniques are used to record the brain activity because recordings from invasive electrodes in the human brain are always restricted for ethical reasons. Non-invasive techniques are much simpler to use and more subjects are available, but they obviously lack in precision and it is difficult to distinguish simultaneously occurring processes. One possibility

is to carry out such experiments with monkeys using invasive techniques, but it still remains unclear if the findings of these experiments can be generalized to humans.

In view of this situation, two goals were set:

1. Investigation of action perception at different levels (intention, goal, kinematics)
2. Quantitative comparison of action perception mechanism between humans and monkeys

The hypothesis of the first aim is that the visual responses of the motor cortex encode observed actions simultaneously along several dimensions and levels of description [2]. To test this, three experiments were designed that allow to decode the responses of actions at different levels. The experiments are based on a GO/NOGO paradigm. In the motor condition, participants (monkeys or humans) are cued a grip type (power, precision, or prehension), after which they have to wait for a second cue that requires them to perform the action (GO) or keep it back and wait for the next trial (NOGO). In the visual condition, they have to observe the experimenter doing the same task. Depending on the level of perception that is to be investigated, different variations are possible. In this Master's thesis, motor and visual responses at the goal level are studied and it will be investigated if the immediate goal of observed actions can be decoded from the visual responses both before and after motion onset. It is hypothesized that this is the case.

For the second aim, the same experimental protocol will be performed on both human (ECoG or SEEG) and monkey (population responses and LFPs) participants. This will allow a direct comparison between humans and monkeys regarding neuronal responses and mechanisms of action perception. In addition, it will be possible to test the assumption that activity in the F5 areas in macaques provides a good model for human action perception.

My contribution to this project will be, in a first part, to analyze the motor responses recorded in monkeys and look out for characteristics specific for frequency bands during movement execution, preparation, and suppression.

These characteristics will then be compared to visual responses in monkeys and humans, at different levels of depth in the motor cortex.

To do so, I will, in a second part, run the experiment with patients at the Boston Children's Hospital. It is crucial that the experiment carried out on human subjects follows the same protocol as it was done on monkeys.

To summarize, the questions that will be explored in this part of the project are: which modulations in the neuronal responses of the motor cortex are characteristic for movement execution, preparation, and suppression? Are they present not only in motor responses, but also in visual responses? Is the intermediate goal of the action (i. e. the grip type) encoded in visual responses? And lastly, are these characteristics preserved between monkeys and humans?

2 Theoretical Background

2.1 Mirror neurons

When we execute an action, certain areas in our brains are active. It has been discovered—originally in the monkey premotor cortex—that groups of neurons also react when the same or a similar action is observed [3–5]. It has been shown that observed actions generalize to species (e. g. a monkey who observes a monkey as well as a human) [6, 7], perspective (first or third person) [6] or distance [7]. Nevertheless, humans are able to distinguish between movements even if these are alike with the exception of minor differences [8–13]. To name a few examples, point lights attached to the shoulder, elbows, wrists, hip, knees, and ankles allow the distinction of female and male walkers to 70 %, and any of these clues seem to be sufficient [8]. According to Johansson, “adequate” combinations of five to ten elements provide enough clues to identify human motion [9]. In social interactions, as Becchio et al. found, movements depend on the intention of both communication partners, not only on the intention of the person carrying out the motion. As the kinematics of one partner adapt to the kinematics of the other, it could be that the partners perceive a behavior and perform it

themselves (that is, a form of mimicry) [10]. According to Barraclough et al., prior experiences have a great influence on action understanding. They showed that endured exposure to visual stimuli resulted in an adaptation of the subject’s own kinematic to hand grasping motion presented in a movie [13].

What are mirror neurons good for? Imitation seems to be a very intuitive functionality of mirror neurons, however, some researchers believe that “true imitation” (not only repeating what is seen but fully understanding the intention and purpose of the action [14]) can only be done by humans and apes [15], so there must be another, older function of mirror neurons.

This other function could be action understanding. When we see someone else doing an action, it’s almost as if we were doing the action by ourselves: the involved neurons are activated in our cortex, and since we know the outcome of those neurons if they are activated, we understand what the other person is doing [16]. There is evidence that this is indeed the case: it has been shown that some mirror neurons become also active when the monkeys hear a sound that they associate with the action (they understand the action but don’t see it) [17], so the activity of those mirror neurons was triggered by the meaning and not by the visual features of the observed action.

In humans, mirror neuron activity usually cannot be recorded at single neuron level, but there are a number of studies that recorded brain activity using non-invasive techniques like EEG (electroencephalography) or MEG (magnetoencephalography) or invasive techniques like ECoG (electrocorticography) or SEEG (stereo EEG), or stimulated the nervous system using TMS (transcranial magnetic stimulation). Already in 1954, Gastaut and Bert found, using EEG, a decrease in power in lower frequency bands not only when the subjects executed an action but also when they observed it [18]. In the decades following this experiment, studies showed that a mirror neuron system is present in humans; and that it is also activated by meaningless movements and encodes not only actions but also the movements that form the action, which does not happen in monkeys [19–21]. If the hypothesis

that only humans can perform “true imitation” holds, these two properties must be crucial for humans to imitate each other.

2.2 Brain Activity in Specific Frequency Bands

Electrical activity in the brain can be analyzed by calculating the power spectral density in frequency bands [22], where most of the information is usually contained in lower frequency bands [23, 24]. Low-frequency bands are traditionally denominated by Greek letters [25] and have different amplitudes [26–28]. The exact definitions are non-uniform in the literature, but for instance Logothetis defines them as such: delta: 0 Hz to 4 Hz; theta: 4 Hz to 8 Hz; alpha: 8 Hz to 12 Hz; beta: 12 Hz to 24 Hz; gamma: 24 Hz to 40 Hz or 24 Hz to 80 Hz [29]. Depending on the frequency band, different neuronal events can be observed [29, 30].

The power in the gamma band increases in the primary motor cortex during motor tasks like reaching [31], reaction-time tasks [32], voluntary muscle contractions [33], or abductions and flexions of different body parts (where peak frequency and bandwidth change with limbs) [34]. Gamma activity correlates with specific cortical functions and behaviors like finger position during slow grasping [35], flexion [36] and other [37] movements as well as with arm [38, 39] and shoulder [39] movements and 2D joystick movements [40]. Generally speaking, in ECoG signals, gamma activity is broadband. Several possible explanations have been proposed for this phenomenon: the phases and frequencies of gamma activity may vary over time, or since each electrode records the average of several neurons, the activities originating from these neurons might all have different frequencies [41].

The above examples point out the importance of gamma band activity, but also other frequency bands carry information. The amplitudes in the alpha and beta bands often change when motion is executed or imagined [33, 42]. For reaching tasks, power decreases were found in alpha and beta bands [31, 41]. This alpha and beta suppression often occurs at the same time as gamma band responses for motor tasks

[33] as well as perception [43]. Beta event-related desynchronization before motion onset, that is in the preparation of movement, was found in the supplementary motor area [41, 44]. Besides that, not only gamma powers increase during cognitive processes but also theta powers: theta oscillations with high amplitude have been observed in the whole human brain during perceptual and cognitive processes [45]. It can therefore be concluded that gamma and theta oscillations interact with each other. Indeed, the phase of lower frequencies, like theta, alpha and beta bands, was found to modulate fast gamma oscillation powers [46–50], a relationship that may allow the coordination of fast processes like movements with slower processes like perception, cognition, and action [47].

Predicting movements out of brain activity can have applications in brain computer interfaces, see for examples the works by Acharya et al. [35], Kubánek et al. [36], Miller et al. [37], Pistohl et al. [38], Schalk et al. [39], or Leuthardt et al. [40].

2.3 Cortical Layers

Motor control is, amongst other higher-order brain functions, processed in the neocortex, which is organized into six horizontal layers [51]. Signals from the environment have to be translated to the brain’s internal representation of the information, which is done in different cortical layers [52]. Both sensory input and prior knowledge of the world are necessary to create an internal representation [53]. According to a common view, each area in the cortex is responsible for specific computations to process the sensory input. To communicate and to eventually “agree” on a representation, feedforward projections signal and transform sensory inputs [54, 55] and generate a “hypothesis”, which, in turn, is compared to and constrained by feedback-derived “priors”, that is, learned representations of the environment [56]. Feedback processing can then lead to a prediction of the environment [54, 55]. The hypothesis is based on the prior knowledge but, at the same time, is set by sensory input. Therefore, there is no start and no end of information flow [57]. Every area can develop one or more hypotheses

without being influenced by its neighbors only [52].

Feedback and feedforward inputs are initiated and terminated in different cortical layers: feedforward pathways originate from layers I to III (most superficial layers) and go to layer IV, whereas feedback inputs originate in the lower two layers and avoid layer IV as target [52] and they have distinct oscillatory rhythms. Examples for the visual cortex: low (≈ 4 Hz and higher (60 Hz to 80 Hz) frequency synchronization is associated with feedforward input, whereas mid-range (14 Hz to 18 Hz synchronization is associated with feedback input [58]; lower (5 Hz to 15 Hz) frequency synchronization is associated with feedback input, whereas higher (40 Hz to 90 Hz [59]) frequency synchronization is associated with feedforward input. It has also been shown that in deep layers, synchronization rather occurs in lower frequency ranges, while more superficial layers rather synchronize in higher frequencies [60–63]. Since feedback processes seem to originate in the deeper layers and feedforward processes in the more superficial layers, this also gives evidence that feedback processes use lower frequencies and feedforward processes use higher frequencies. Most of these examples were studied in the visual cortex, but internal processing in the motor cortex has shown to be similar to other cortical areas [64].

Coding the information in different frequency ranges allows the brain to ponder sensory input with internal information, depending on the situation, because the two types of information can be passed along independently [52]. The given distribution of frequencies—feedforward: rather high frequencies, feedback: rather low frequencies—intuitively seems to make sense: the environment can change fast, processing sensory input has to be done at a high rate. However, previously learned priors are generally more stable and should not be influenced from environmental changes as quickly.

3 Monkey LFP

3.1 Background

Local Field Potentials (LFPs). In the monkey, the electric potential was measured with small electrodes in the brain and it is referred to as a local field potential (LFP). LFPs contain information about deeper location in the brain than, for example, ECoG, which records activity on or close to the cortical surface [65], but are spatially less specific and have a lower selectivity for stimuli than neuronal spiking activity (MUA) [66]. Briffaud et al. found that high amplitude waves of the LFP signal correlate with single-cell recordings [67]. Sometimes the precision of LFPs is comparable to or even surpassing single-cell precision [68, 69].

To analyze the filtered, noise-less LFP signals, a spectrogram can be helpful to determine LFP frequency, amplitude and other characteristics [24]. Supposedly, only a few (low) frequency ranges are informative [23, 30, 70, 71] (see Section 2.2 for more).

3.2 Materials and Methods

3.2.1 Data Collection

The data has been collected by Dr. Antonino Casile³ at Harvard Medical School (Department of Neurobiology, Boston, MA, USA). The data used in this work was recorded from an adult male rhesus monkey (*Macaca mulatta*) weighing 9.8 kg with two multi-site linear electrodes (V-Probe, 16 channels each, 150 μm spacing between the channels, Plexon Inc., Dallas, TX, USA) in the motor cortex (F5 area). The two electrodes were placed $\sqrt{2}$ mm apart.

3.2.2 Task

The monkey was trained to perform the same motor task as described in Section 4.2.2, only that the board had smaller dimensions (prehension: a thin circular plate with diameter 3.5 cm and height 1.2 cm; precision: a rectangular plate with side lengths 0.5 cm \times 0.8 cm \times 0.5 cm;

power grip: cylinder with diameter 4 cm and height 2.5 cm, see (Caggiano et al., 2015) [6]).

For the visual task, the experimenter executed the motor task in front of the monkey. The monkey could see the cue lights that determined the object to grab and could hear the sound that determined the GO/NOGO condition. It has been found that the most important features to attract the initial attention of the monkey was the experimenter’s face or the goal object [72], so the trial was started when the monkey was gazing at one of those features. The monkey did not move during the trials.

In both the motor and the visual task, the time stamps of important events (turning on and off the cue and the sound, lifting the arm, touching the object, putting the arm back to the resting plate, and the reward at the end of a successful trial) were recorded along with neuronal signals to allow an alignment of the events with the neuronal activity.

3.2.3 Data Analysis

The data was analyzed with custom scripts written in Matlab (Mathworks, Natick, MA, USA, version R2018b) using the Chronux toolbox [73]. Signals were recorded at a sampling rate of 30 kHz. They were bandpass-filtered (second-order bandpass filter with passband 0.1 Hz to 100 Hz) and notch-filtered at frequency 60 Hz. For each trial and channel, the signal was aligned with a certain event (usually with the cue for NOGO trials, with the hand-object contact for motor GO trials and with the arm lift for visual GO trials) and a large interval of up to 7 s before and 6 s after the event was extracted. Only correct trials were included. Abnormally distributed trials (trials where the kurtosis differed more than two standard deviations from the mean kurtosis over all trials) and outliers (trials where the mean absolute value differed more than two standard deviations from the absolute mean over all trials) were rejected. Table 1 and Table 2 show the number of remaining trials used for further analysis.

Time-frequency analysis. A multi-taper time-frequency spectrum with 5 tapers, a time-

³Currently: Center for Translational Neurophysiology, Istituto Italiano di Tecnologia, Ferrara, Italy

Motor	GO	NOGO
Prehension	E2: 14 to 15, E3: 14 to 15	E2: 12 to 13, E3: 12 to 13
Precision	E2: 21 to 22, E3: 21 to 24	E2: 16, E3: 15 to 16
Power	E2: 14 to 15, E3: 16	E2: 17 to 18, E3: 18 to 19
All	E2: 50 to 53, E3: 51 to 53	E2: 45 to 46, E3: 44 to 46

Table 1: Number of trials in the motor task that remained after removal of artifacts, depending on the channel.

Visual	GO	NOGO
Prehension	E2: 24 to 27, E3: 24 to 28	E2: 17 to 19, E3: 16 to 18
Precision	E2: 22, E3: 20 to 22	E2: 23, E3: 22 to 23
Power	E2: 20 to 22, E3: 20 to 23	E2: 22 to 24, E3: 22 to 24
All	E2: 66 to 70, E3: 63 to 70	E2: 67, E3: 64 to 67

Table 2: Number of trials in the visual task that remained after removal of artifacts, depending on the channel.

bandwidth product of 3, a window size of 0.75 s and a step size of 0.075 s was computed and converted to decibel. For each trial, the baseline was subtracted. The baseline was defined as the average over time in the interval of 0.6 s to 0.1 s before the cue. For each spectrogram, the average over trials was calculated and plotted.

There were two electrodes with 16 channels each and four experimental conditions (GO trials and NOGO trials, and motor and visual responses, which gives four combinations). All channels and conditions were analyzed separately. In the first part of the analysis, the average of all three grip types was taken, in the second part the grip types were treated separately as well.

In order to emphasize certain observations, the average power in a mid-frequency range (15 Hz to 25 Hz) and in a high-frequency range (40 Hz to 60 Hz) was taken and plotted against time for all four conditions (for a representative example channel).

Average power vs. channel depth. To quantify the results, the sum of the power in interesting frequency (0.1 Hz to 8 Hz, 15 Hz to 25 Hz, and 40 Hz to 60 Hz) and time ranges (500 ms after the cue and the go signal and around touch and release of the object) was taken and plotted against the channels of each electrode, where channel 1 was the most superficial and channel 16 the deepest channel.

The Pearson correlation coefficient was calculated and, in case of a significant correlation at level $\alpha = 0.05$, the regression line was computed and plotted as well.

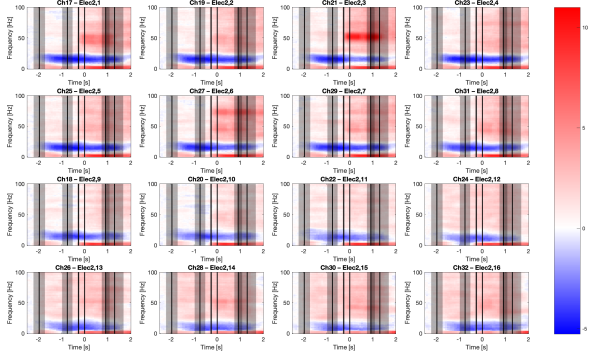
Distinction score vs. channel depth. To estimate the effect of channel depth on the ability to distinguish between grip types, the average power in a time-frequency rectangle was taken for each condition, electrode and channel, which resulted in a value for each trial. For a certain experimental condition and channel, this “trial vector” of one grip type was compared to another grip type using Student’s unpaired t-test at significance level $\alpha = 0.05$. Given that there are three grip types, there are three possible combinations of grip types. The number of positive t-tests assigns a “distinction score” to each experimental condition and electrode.

To estimate the linear correlation between the distinction score and the depth of a channel, the Pearson correlation coefficient was computed as well as the statistical significance at level $\alpha = 0.05$.

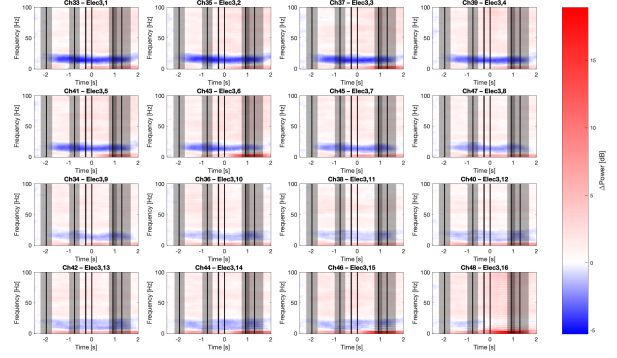
3.3 Results

3.3.1 All Trials

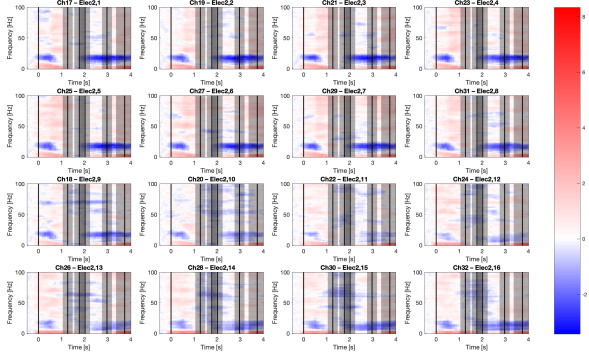
Time-frequency analysis. As a first step, the temporal evolution of the power of the LFPs from two electrodes (16 recording sites each)



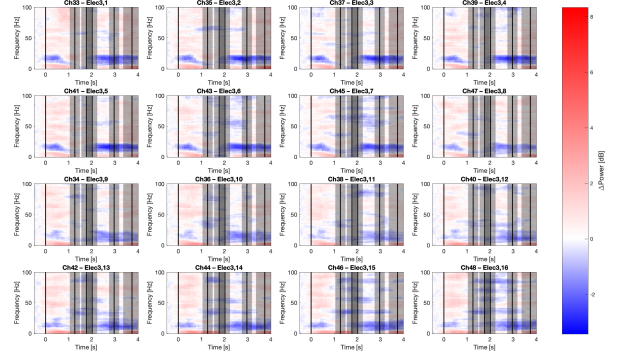
(a) Electrode 2, GO trials.



(b) Electrode 3, GO trials.



(c) Electrode 2, NOGO trials.



(d) Electrode 3, NOGO trials.

Figure 1: Time-frequency analyses of the motor responses from every channel on the two electrodes, GO and NOGO trials. Average of all trials without distinction between the grip types. The plots on the top left of each panel correspond to the most superficial channel, plots on the bottom right to the deepest channel. NOGO trials were aligned with CueOn and GO trials were aligned with ObjTouch (time $t = 0$ s). The vertical black lines correspond to the average time of the occurrence of the events in the order: CueOn, GoSignal, ArmLift, ObjTouch, ObjRelease, RewardUp, the black shade being the standard deviation. For NOGO trials, the events from ArmLift to ObjRelease are virtual.

in the motor cortex of a monkey (F5) during the execution of a grasping task (motor task) or the observation of the same task (visual task) was investigated in order to develop a feeling which frequency bands encode important information with respect to reaching and grasping movements, as well as the preparation and suppression of them. To give an overview over the different channels and electrodes in both conditions, power spectra of the LFPs were calculated by a multitaper time–frequency analysis. Fig. 1 shows the modulation from the baseline, which was defined as the interval from 600 ms to 100 ms before the cue, for both electrodes and both conditions with increasing depth (with the most superficial channel on the top left). The vertical black lines correspond to

the average time across trials (with standard deviation) of the events as the experiment enrolled (see caption). For NOGO trials, the events from ArmLift to ObjRelease did not take place and the vertical lines correspond to an estimation of the times at which the movement might have been carried out in the case of a GO trial. Time $t = 0$ corresponds to ObjTouch in GO trials and to CueOn in NOGO trials.

The execution and preparation of an action seems to result in at least three noticeable changes with respect to the baseline. In a low-frequency range (0.1 Hz to 8 Hz), power increases can be observed at different events, which seems to be dependent on conditions and electrode depth. For GO trials, the power increase starts at CueOn and intensifies at

ObjTouch and **RewardUp**. In the deeper channels of electrode 2 (Fig. 1a), **RewardUp** seems to become more important, whereas on electrode 3 (Fig. 1b), the power becomes stronger in the most superficial and deepest channels during the movement period. In **NOGO** trials (Fig. 1c and 1d), the power is a little higher at **CueOn** and **RewardUp** but gets close to baseline level during the virtual movement period.

In a mid-frequency range (15 Hz to 25 Hz), there is a prominent negative band right after the cue is turned on, which is interrupted in the **NOGO** trials (Fig. 1c and 1d), this time between **CueOn** and **GoSignal**, and it reappears at the estimated moment at which **ObjTouch** would have taken place in **GO** trials (virtual **ObjTouch**). Fig. 2 shows the average power in the frequency band in question as the trial enrolled, recorded from one representative channel (third most superficial on electrode 2). **GO** trials (blue, lower x-axis) were aligned with **ObjTouch** and **NOGO** trials (red, upper x-axis) with **CueOn**. It can be seen that in **NOGO** trials, the power in this range drops right after **CueOn**, rises back to baseline level and beyond, before it starts to drop again between **CueOn** (left vertical line) and virtual **ObjTouch** (around **GoSignal**). At virtual **ObjTouch** (right vertical line), it is at about the same level as the **GO** trials. Given the high variance across trials, these observations might not be statistically significant, but there is a clear tendency.

In a high-frequency range (40 Hz to 60 Hz), an increase in power occurs after **ArmLift** for electrode 2 in the **NOGO** trials (Fig. 1a). This is more clear when taking the average power in this frequency range: in Fig. 3, we can see that the power (again from the third most superficial on electrode 2) in particular reaches a local maximum when the object is touched (middle vertical line), drops a little while the object is touched and rises again to an even higher level shortly before the object is released (right vertical line). Note that the interesting part of the trial ended in average approximately 280 ms after **ObjRelease**. The increase in power after **ObjRelease** is probably due to the reward the monkey was given and other movement, which is not relevant. The increase at (virtual) **ObjTouch** is not present in the **NOGO** trials (see

also Fig. 1c). Electrode 3 doesn't seem to have this prominent patch either (Fig. 1b), but when comparing to the **NOGO** trials (Fig. 1d), it can be seen that here, the power rather shifts to negative for some frequencies and not to the positive.

With increasing depth, these features have a tendency to become less prominent, that is, the power modulation is closer to zero for most features in the deeper channels, with exception of the red low-frequency band (especially for electrode 3 and **NOGO** trials).

Fig. 4 shows the same plots for the visual responses. Here, the **GO** trials are aligned with the **ArmLift** event. Comparing the motor responses to the visual responses, it can be noticed that generally speaking, the modulations of the power from the baseline are weaker. Nevertheless, the same features can be detected.

In the low-frequency band, the increases in power often already occur at **ArmLift** and the

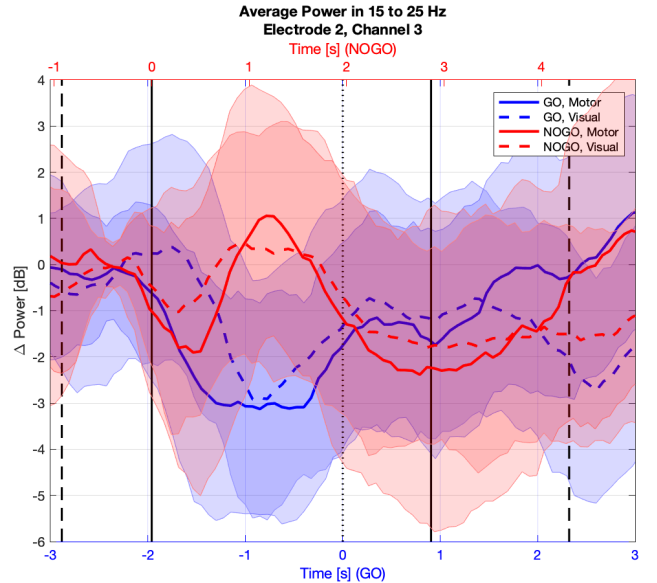


Figure 2: Average power recorded by the third most superficial channel of electrode 2 in the frequency band 15 Hz to 25 Hz with respect to the baseline for motor and visual responses. **GO** trials are aligned at **ObjTouch** (blue, time line: lower x-axis), **NOGO** trials are aligned at **CueOn** (red, time line: upper x-axis). The vertical lines from left are: (dashed) visual **CueOn**, (solid) motor **CueOn**, (dotted) motor and visual **ObjTouch**, (solid) motor **ObjTouch**, (dashed) visual **ObjTouch**, all mean values and with respect to the **GO** trials.

decreases between **ObjTouch** and **ObjRelease** are more outstanding (Fig. 4a and 4b). For electrode 2, there seems to be a shift from **ArmLift** to **ObjTouch** in the deeper channels for the first considerable power increase. In **NOGO** trials however, the red band disappeared, instead, there are even power decreases starting around **GoSignal** (Fig. 4c and 4d).

In the mid-frequency band, the negative modulation also occurs in **GO** trials, but only at **ArmLift** when the monkey’s attention was caught by the movement (Fig. 4a and 4b), whereas in the motor trials, it already occurred at **CueOn**. Fig. 2 clearly shows that the power in motor and visual trials behaved in a very similar way (note that the visual trials were in general executed more slowly, hence the discrepancy in the last plotted second).

In the high-frequency band, the increase in power after **ObjTouch** in **GO** trials are not as clear but still present, especially in the more

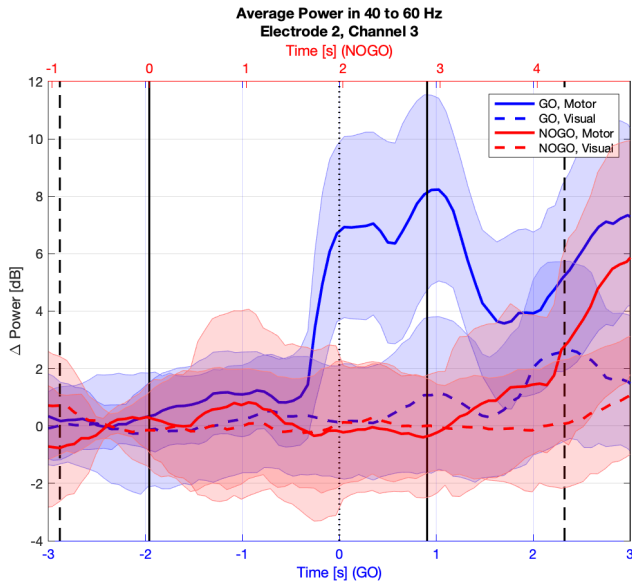


Figure 3: Average power recorded by the third most superficial channel of electrode 2 in the frequency band 40 Hz to 60 Hz with respect to the baseline for motor and visual responses. **GO** trials are aligned at **ObjTouch** (blue, time line: lower x-axis), **NOGO** trials are aligned at **CueOn** (red, time line: upper x-axis). The vertical lines from left are: (dashed) visual **CueOn**, (solid) motor **CueOn**, (dotted) motor and visual **ObjTouch**, (solid) motor **ObjTouch**, (dashed) visual **ObjTouch**, all mean values and with respect to the **GO** trials.

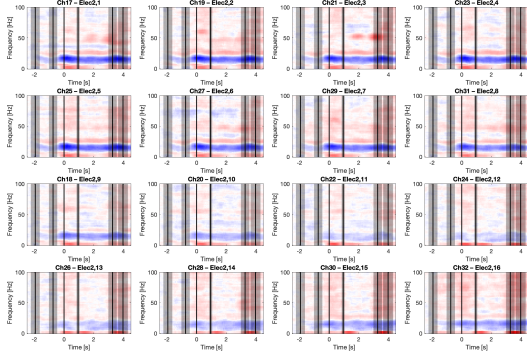
superficial channels on electrode 2 (Fig. 4a). At the same time, the higher frequencies are more similar to the baseline (modulations closer to zero, sometimes even negative) after **ObjTouch** in the **GO** trials, somewhat resembling the **NOGO** trials of the motor responses (Fig. 1c and 1d).

When comparing the visual average power in the high frequency band, it again behaves in a similar way as the motor responses, only much weaker and with a delay. This is not only due to the more slowly executed task because in the motor response, the maximum is already reached at **ObjTouch**, in the visual response however about one second after the touch. The second maximum however occurs at the same event in both conditions.

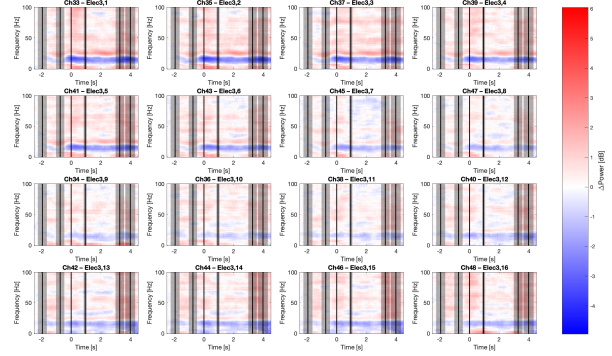
Summed up Power in Varying Depth In an attempt to quantify these observations, the values in the time-frequency plot were summed up in rectangles of interest (that is, specific frequency and time ranges). The results were plotted against electrode depth (where 1 corresponds to the most superficial and 16 to the deepest channel) in Fig. 5 and 6 for motor and visual responses respectively. Then, the Pearson correlation between summed up power and channel depth was calculated. If it was statistically significant at $\alpha = 0.05$, a regression line was plotted.

The frequency ranges of interest were, as before, a low-frequency range of 0.1 Hz to 8 Hz, a mid-frequency range of 15 Hz to 25 Hz, and a high-frequency range of 40 Hz to 60 Hz. The time ranges of interest were 500 ms around the events **CueOn**, **GoSignal**, **ObjTouch**, and **ObjRelease**.

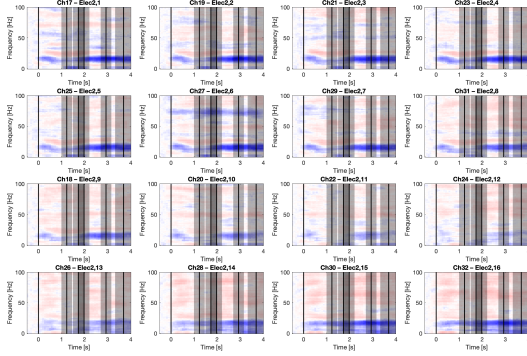
First, let’s have a look at the motor responses in Fig. 5. In the mid-frequency range, the power is the most negative in the most superficial channel and tends towards baseline level with increasing depth. This is true for all time ranges and both electrodes in the **GO** condition, and for all time ranges in the **NOGO** condition except the 500 ms after **GoSignal**, where the power recorded with electrode 3 is negatively correlated with depth, that is, it becomes more negative at greater depth, and electrode 2 is not significantly correlated.



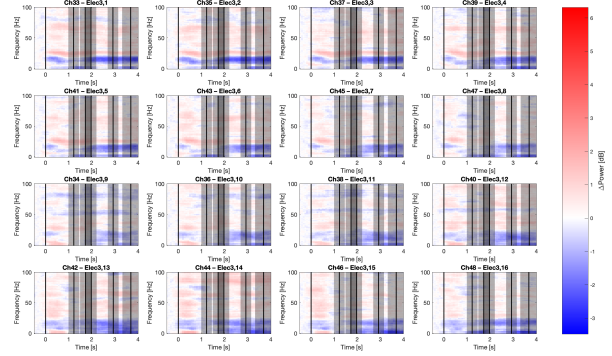
(a) Electrode 2, GO trials.



(b) Electrode 3, GO trials.



(c) Electrode 2, NOGO trials.



(d) Electrode 3, NOGO trials.

Figure 4: Time-frequency analyses of the visual responses from every channel on the two electrodes, GO and NOGO trials. Average of all trials without distinction between the grip types. The plots on the top left of each panel correspond to the most superficial channel, plots on the bottom right to the deepest channel. NOGO trials were aligned with CueOn (time $t = 0$ s) and GO trials were aligned with ArmLift (time $t = 0$ s). The vertical black lines correspond to the average time of the occurrence of the events in the order: CueOn, GoSignal, ArmLift, ObjTouch, ObjRelease, RewardUp, the black shade being the standard deviation. For NOGO trials, the events from ArmLift to ObjRelease are virtual.

In the high-frequency range, the movement preparation power (time after CueOn) is positive and increases with depth in both GO trials and NOGO trials. During the movement itself, the power is positive in the GO condition and rather negative in the NOGO condition and has a tendency to decrease with depth, even though it is not always a significant correlation.

In the low-frequency range, the positive power from electrode 2 has a strong tendency to decrease with depth during the movement period. Electrode 3 often behaves in the opposite way.

For the visual responses in Fig. 6, the results are less clear. In the mid-frequency range, the power from electrode 2 also increases towards zero with greater depth in almost all time

ranges of the GO condition, electrode 3 however is either not linearly correlated (for instance in the time window around ObjTouch, the power gets close to baseline for the channels in the middle but is negative for both deep and superficial channels) or the power decreases with depth. In the NOGO condition, the power has a tendency to increase to baseline with depth during the preparation period and has a tendency to decrease after GoSignal (which of course is a NOGO signal in this case).

In the high-frequency range, almost no significant correlations exist, but in the GO condition there is an overall tendency to increasing power with depth during preparation and decreasing power during execution, similar as in the motor condition. In the NOGO condition,

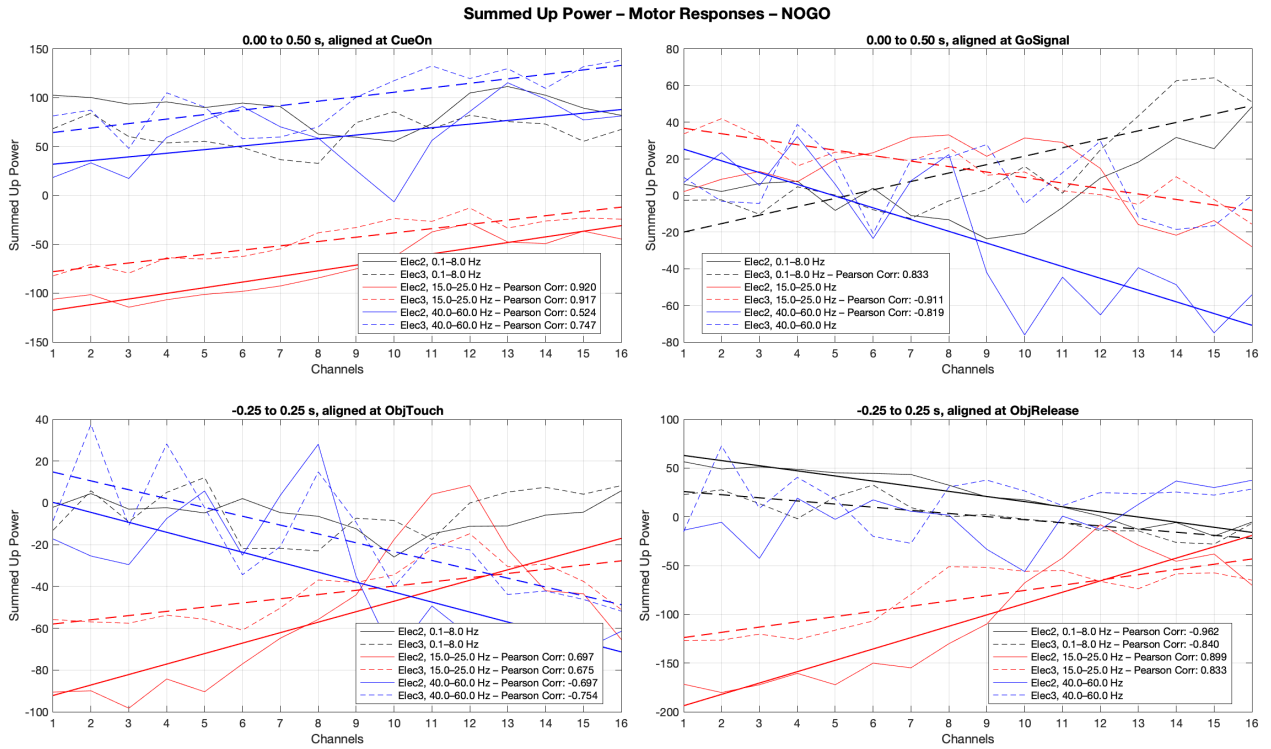
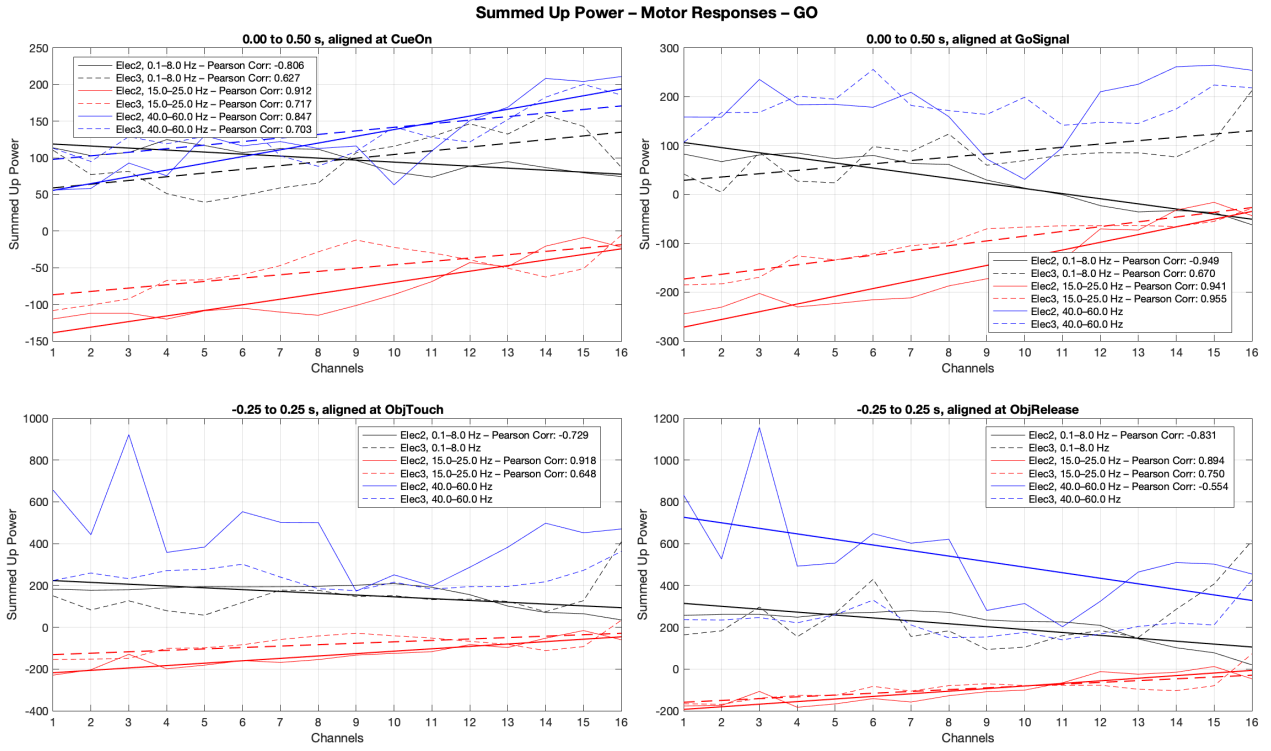


Figure 5: Summed up power of the motor responses in time and frequency ranges of interest. The bold lines correspond to the linear regression of the summed up power with electrode depth (see legend for Pearson correlation coefficient). If there is no line, the correlation was not significant. 1 is the most superficial, 16 the deepest channel.

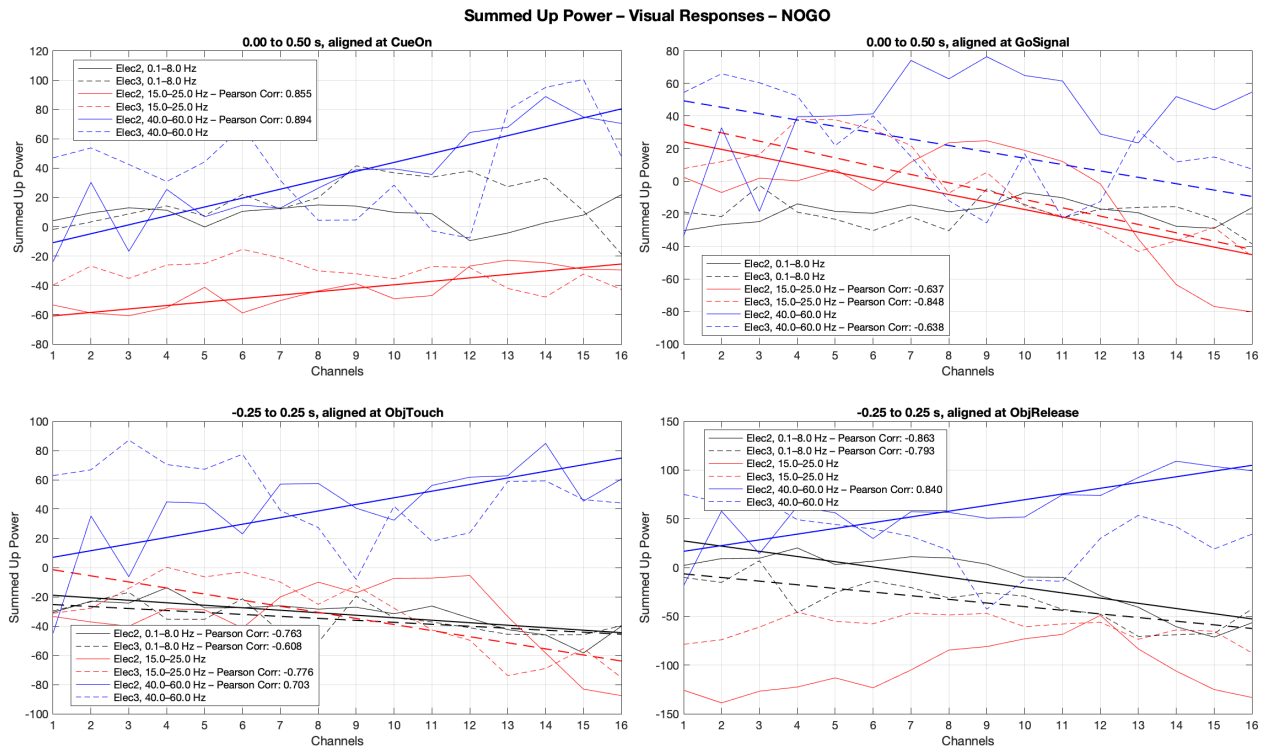
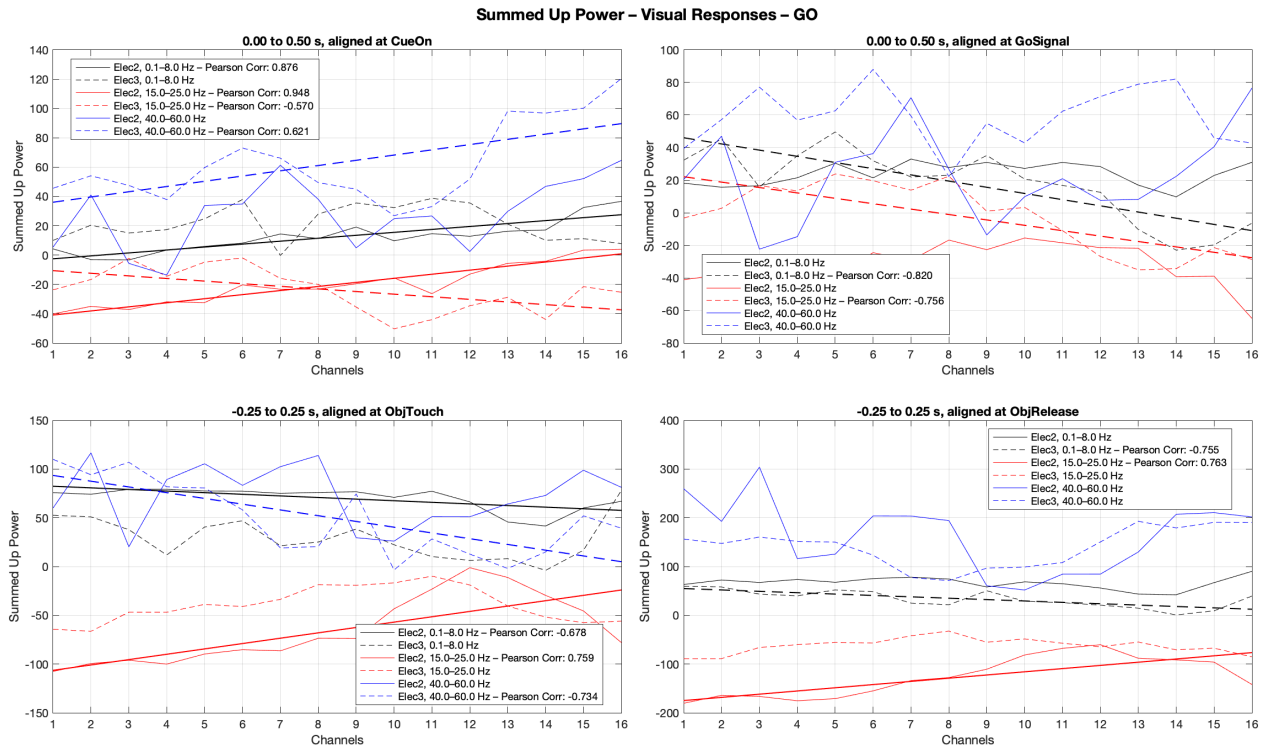


Figure 6: Summed up power of the visual responses in time and frequency ranges of interest. The bold lines correspond to the linear regression of the summed up power with electrode depth (see legend for Pearson correlation coefficient). If there is no line, the correlation was not significant. 1 is the most superficial, 16 the deepest channel.

the power always increases with depth (except after `GoSignal`), which is different from the motor condition.

In the low-frequency range, there are only a few significant correlations too, again with a tendency to increasing power during movement preparation and decreasing power during the movement in both GO and NOGO condition, quite similar to the motor condition.

3.3.2 Trials by Grip Types

Time-frequency analysis. The goal of the next step was to see if and in which frequency bands the grip type is encoded for different times as the experiment enrolled. The spectrograms in this section were obtained in the same way as those in the previous section, but this time, the trials for each grip type were plotted separately.

As an example, the third most superficial channel from electrode 2 for both motor and visual responses is shown in Fig. 7. The red patches in frequency band 40 Hz to 60 Hz are present in all grip types (motor responses, Fig. 7a) but distinguishable by eye, especially the precision grip seems to evoke a smaller increase in power than the other two. The movement of the arm and fingers seems to be encoded in this frequency band: in Fig. 8, the average power between 40 Hz and 60 Hz was plotted and it can be seen that the power increases right at `ArmLift` (which starts on average about 260 ms before `ObjTouch`), drops a little while the monkey was holding the object and rises again before the object was untouched, probably when the monkey started to move the fingers. This figure also shows that the power increases to a different extent for the grip types: at `ObjTouch`, the power rises to the highest level for prehension grip, followed by power and precision. The action of releasing the object however seems to be very similar for all grip types.

The negative band between frequencies 15 Hz to 25 Hz is particularly stronger between `CueOn` and `ArmLift` for precision as compared to prehension and power (Fig. 7a). The information encoded here might correspond to the preparation of the movement, as differences be-

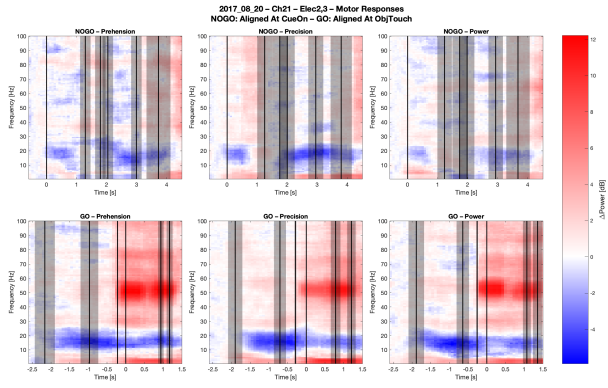
tween grip types are most prominent at `CueOn`, and the blue band is interrupted at that time in the NOGO trials.

One can also note that the NOGO trials vary from one grip type to the other as well, suggesting that the suppression or inhibition of a motion is considered as “motion” from the brain.

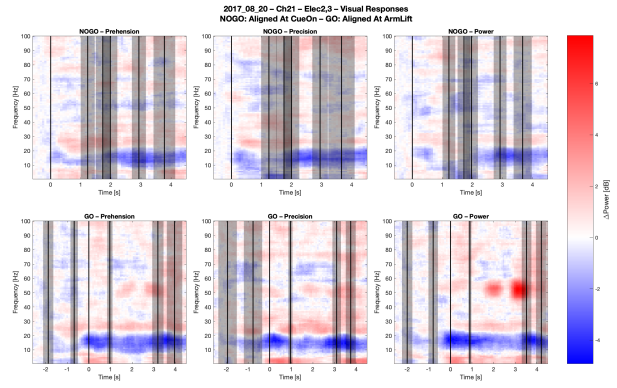
Similarly, those movement-related features can be found in the visual responses in Fig. 7b, to a much smaller scale, but distinguishable in terms of grip type. It is to notice that the red patches in frequency band 40 Hz to 60 Hz seem to occur later, after `ObjTouch`, as if the monkey needed some time to realize it was this motion. Also, as can be seen more clearly in the right panel of Fig. 8, power grip is the most distinguishable from the other two, but the responses for the three grip types are very close to each other.

Pearson Correlations. To explore in more detail how the power is related to electrode depth, the average power in certain time and frequency ranges was taken for each trial for each condition, task, electrode channel, and grip type. The thusly obtained values were tested using Student’s unpaired t-test to check if the hypothesis that the average over trials for one grip type is the same for another grip type can be rejected. For every channel, the amount of rejected t-tests was counted. As there are three possible combinations, every channel can score up to three, implying that this channel would be very good in distinguishing between grip types. The results are summarized in Tables 3, 4, 5, and 6, where the distinction score of the best channel was indicated for motor and visual and GO trials and NOGO trials respectively. It is to be noted that in general, the low-frequency range seem to be the best to predict the grip type, especially in the motor condition (Tables 3 and 4). In the visual condition, NOGO trials (Table 6) are in general better doing better than GO trials (Table 5).

Then, the Pearson correlation between this score and the channel depth was calculated and the results were plotted in Fig. 9. Statistically significant correlations at $\alpha = 0.05$ were marked with an asterisk.



(a) Motor responses.



(b) Visual responses.

Figure 7: Time-frequency analyses of both the motor and visual responses from the third most superficial channel on electrode 2, GO and NOGO trials and the three grip types. Average of all trials. NOGO trials for both tasks were aligned with *CueOn*, motor GO trials were aligned with *ObjTouch* and visual GO trials were aligned with *ArmLift* (time $t = 0$ s). The vertical black lines correspond to the average time of the occurrence of the events in the order: *CueOn*, *SignalOn*, *ArmLift*, *ObjTouch*, *ObjRelease*, *RewardUp*, the black shade being the standard deviation. For NOGO trials, the events from *ArmLift* to *ObjRelease* are virtual.

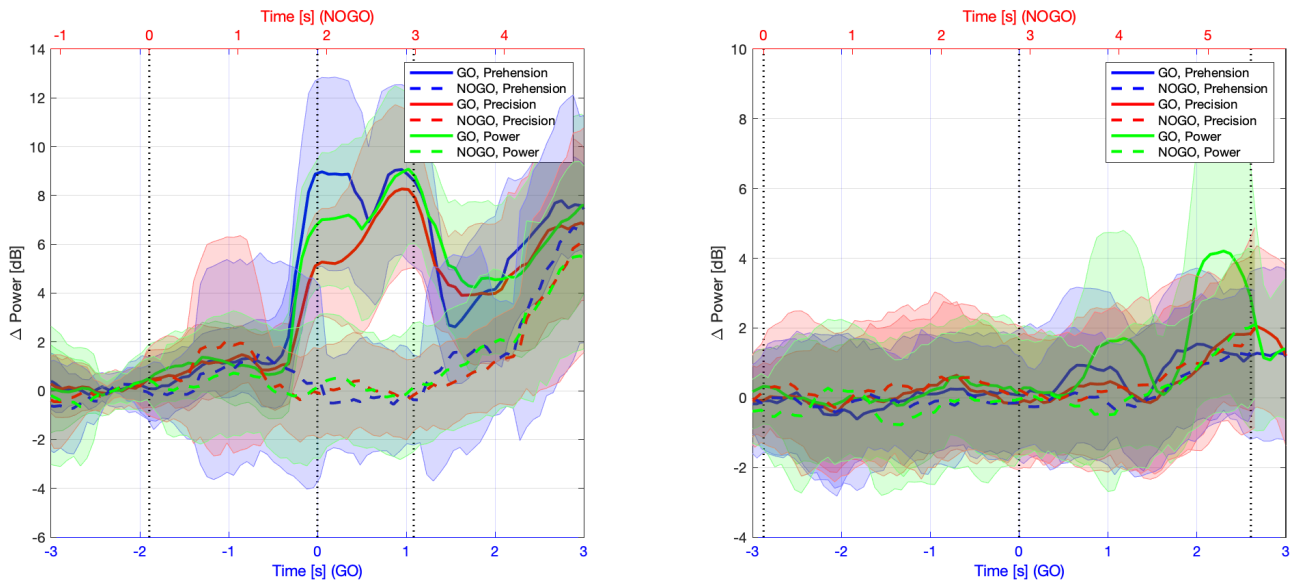


Figure 8: Average power recorded by the third most superficial channel of electrode 2 in the frequency band 40 Hz to 60 Hz with respect to the baseline for motor (left panel) and visual (right panel) responses. GO trials are aligned at *ObjTouch* (blue, time line: lower x-axis), NOGO trials are aligned at *CueOn* (red, time line: upper x-axis). The vertical lines in both panels correspond to (left) *CueOn*, (middle) *ObjTouch*, (right) *ObjRelease*, all mean values and with respect to the GO trials.

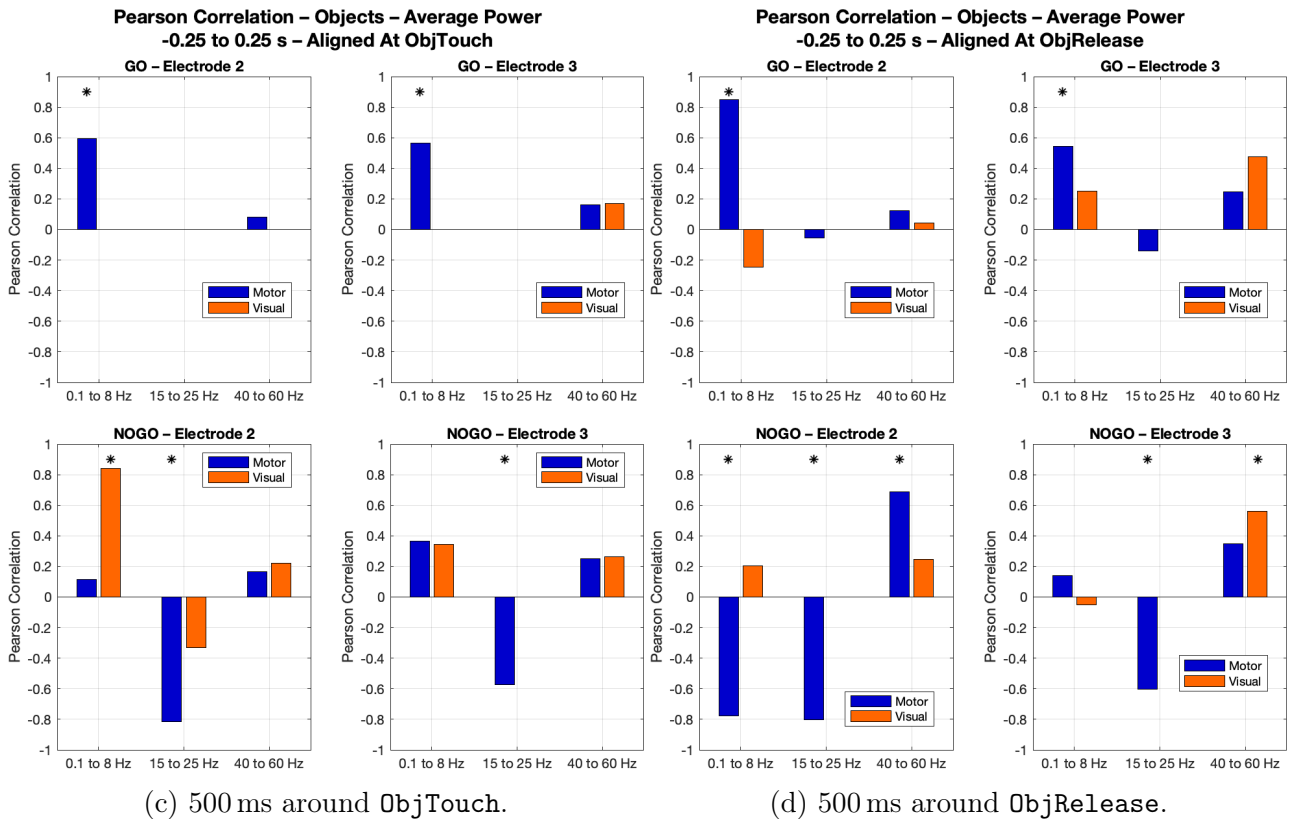
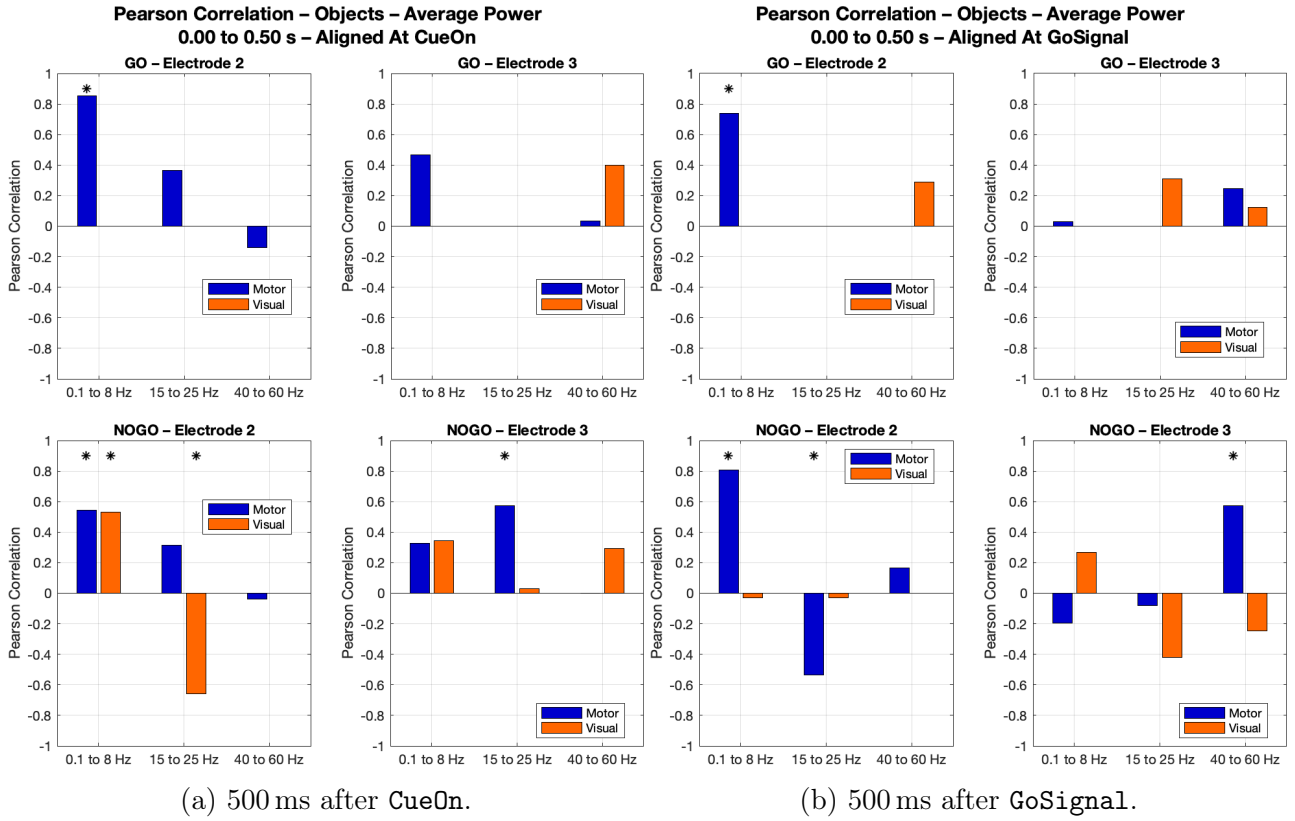


Figure 9: Pearson correlation coefficient for motor and visual responses between channel depth and grip type distinction score for different time and frequency ranges. A positive correlation means that the deeper channels can better distinguish between the grip types, a negative correlation that the more superficial channels are better in doing so. An asterisk marks statistically significant correlations ($\alpha = 0.05$).

Motor GO	0.8 to 10 Hz	15 to 25 Hz	40 to 60 Hz
CueOn	E2: 3 E3: 2	E2: 1 E3: 0	E2: 1 E3: 2
GoSignal	E2: 3 E3: 1	E2: 0 E3: 0	E2: 0 E3: 2
ObjTouch	E2: 2 E3: 2	E2: 1 E3: 1	E2: 2 E3: 2
ObjRelease	E2: 2 E3: 1	E2: 0 E3: 0	E2: 2 E3: 1

Table 3: Maximum distinction score for motor responses, GO trials.

Motor NOGO	0.8 to 10 Hz	15 to 25 Hz	40 to 60 Hz
CueOn	E2: 2 E3: 2	E2: 2 E3: 1	E2: 2 E3: 2
GoSignal	E2: 1 E3: 1	E2: 1 E3: 1	E2: 1 E3: 1
ObjTouch	E2: 3 E3: 3	E2: 2 E3: 2	E2: 2 E3: 2
ObjRelease	E2: 2 E3: 1	E2: 2 E3: 1	E2: 1 E3: 2

Table 4: Maximum distinction score for motor responses, NOGO trials.

Visual GO	0.8 to 10 Hz	15 to 25 Hz	40 to 60 Hz
CueOn	E2: 0 E3: 0	E2: 0 E3: 0	E2: 0 E3: 1
GoSignal	E2: 0 E3: 0	E2: 0 E3: 1	E2: 1 E3: 2
ObjTouch	E2: 1 E3: 1	E2: 0 E3: 0	E2: 1 E3: 2
ObjRelease	E2: 0 E3: 0	E2: 0 E3: 0	E2: 0 E3: 2

Table 5: Maximum distinction score for visual responses, GO trials.

Visual NOGO	0.8 to 10 Hz	15 to 25 Hz	40 to 60 Hz
CueOn	E2: 2 E3: 2	E2: 1 E3: 1	E2: 0 E3: 2
GoSignal	E2: 1 E3: 2	E2: 1 E3: 0	E2: 0 E3: 2
ObjTouch	E2: 2 E3: 1	E2: 0 E3: 0	E2: 2 E3: 2
ObjRelease	E2: 1 E3: 2	E2: 1 E3: 0	E2: 2 E3: 2

Table 6: Maximum distinction score for visual responses, NOGO trials.

There is only one case where both the motor and the visual responses lead to a significant correlation for the same conditions: in electrode 2, for NOGO trials in the low-frequency range after CueOn, we have a positive correlation between the distinction score and channel depth. For motor responses, there is always a positive correlation in this frequency band, except in the NOGO trials around ObjTouch and ObjRelease. For the mid-frequency range, there are no correlations in the GO trials, but negative correlations in the virtual movement time span in electrode 2 for the NOGO trials in the motor condition. In the high-frequency range, almost no significant correlations can be observed.

3.4 Discussion

3.4.1 Time-Frequency Analysis

In the first part of this project, time-frequency power spectra in a cued GO/NOGO paradigm were analyzed in terms of features specifically related to reaching and grasping movement. Characteristic patterns were found in three frequency ranges: 0.1 Hz to 8 Hz, 15 Hz to 25 Hz, and 40 Hz to 60 Hz.

15 Hz to 25 Hz power drop is related to movement preparation and execution, and is interrupted in NOGO trials. It has been known for a very long time that voluntary movements and the preparation of them block oscillations in the motor area in frequency bands around 15 Hz to 25 Hz (in the literature,

this frequency band is referred to as “beta band” [25] and its exact definition depends on the authors); the first reference dates back to as early as 1949 [74]. Numerous studies could replicate this effect for motor tasks, for example [75–78]. A decrease in power relative to baseline is often considered as an event-related desynchronization [79]. Khanna and Carmena suggest that in order to generate patterns that are specific to preparation and execution of motions, beta oscillations have to be stopped [75]. In GO/NOGO paradigms, this decrease in beta power could also be observed in NOGO trials [77, 78, 80, 81], that is, even when the movement was not executed but only cued, the beta power relative to the baseline became negative, which is in accord with the present work.

Kühn et al. showed in their study that in NOGO trials, the beta power decreased after the NOGO signal just like in the GO trials, but it increased back to normal level faster than in GO trials. More precisely, it restored after the average reaction time in GO trials [77]. The power spectrograms in this work, such as Fig. 1 and 2, also show a recovery of the beta power to baseline level, though it takes place earlier and is already back to baseline level before the go signal (which was signalled by switching off the white noise at the same time as GoSignal would have taken place in the case of a GO trial). It has to be noted though that the information if it was a GO or a NOGO trial in my task was already given at CueOn, that is, when the target was specified. In [77], subjects did only know if they have to press the button or not at the GO/NOGO signal. therefore, in both cases, beta power seems to increase again some time after receiving the information of condition NOGO, possibly stopping the preparation of movement because it was unnecessary. However, in the present work, the beta power drop reappears at the approximate time when the participant would have started the motion in the case of a NOGO trial (ArmLift). It is unclear what lead to this reappearance. The motor tasks for time-frequency analyses involving GO/NOGO paradigms in previous studies (like [77, 78, 80, 81]) are typically much shorter, including tasks like pressing a button with the hand already

very close to the target, which can be done so quickly—in some cases the subjects were even instructed to do the task as fast as possible—that it would be difficult to distinguish between motion onset and offset and there would not be enough time to investigate changes in power during motion. Also, in some studies the beta power drop was present in NOGO trials but in general higher than in the GO condition [77, 78], which could be a similar but less pronounced temporary beta power recovery effect.

A possible explanation of the power drop reappearance could be that the participant imagines the movement even though it is not executed. Lange et al. showed that motor imagery leads to similar results as actually executing the motion. In this study, subjects were presented drawings of hands at different rotations and had to indicate if it is a right or a left hand, therefore the subjects imagined to turn the hand. The time-frequency spectrograms showed the same beta power drop as those of actual movements [82]. Therefore, the monkey in the present task might at first have prepared the movement at CueOn (beta power drop), stopped the preparation (beta power back to baseline) but then he nevertheless imagined the movement he was not supposed to do (“white bear phenomenon” [83]).

40 Hz to 60 Hz power increase is related to motion and is specific for grip types.

It has been shown many times that power increases in higher frequencies (often referred to as “gamma band”, usually defined as some band between 40 Hz and 100 Hz or higher) occur during movement [33, 34, 37, 40, 84–88]. This is in accord with the results of this work. Furthermore, when looking at individual grip types separately (see Fig. 3), it can be seen that the power is strongest at ObjTouch (starts to increase at motion onset), decreases (supposedly when the fingers are at rest, touching the object) and becomes stronger again towards the end of the motion (strongest at ObjRelease and starts to increase before). A similar phenomenon was observed in [31], which also was a self-paced reaching task, in both EEG (non-invasive electroencephalography) and ECoG (electrocorticography).

Power increases again for all conditions (motor and visual, GO and NOGO), when the monkey received a reward, which happened in all cases and induced motion as well (e. g. swallowing).

Power increase in gamma bands therefore seems to be highly associated with motion, as it was induced with the actual movement of the arm or the fingers.

Looking at each grip type separately, one can tell by eye that the different grips evoke a different pattern (Fig. 7). Indeed, Kubánek et al. found different activities in the gamma band for different fingers and finger flexions and could predict the flexion trace with ECoG features [36]. There are two possible views on this. It could be that different movement types require different efforts and therefore lead to different power outbursts. Another explanation could be found when we consider the placement of the electrodes. Previous studies found that gamma activity is spatially more focal in the brain [37, 87], in other words, the information in the gamma frequencies for a movement type is more specific to a certain brain area. The electrode, which keeps its location for all trials, would record a weaker or more diffused signal if a certain movement type activates a more distant brain region than the others. This can also be the reason why those power increases seem to be absent in electrode 3, even for the GO trials (Fig. 1b and 4b). The two electrodes are quite distant from each other ($\sqrt{2}$ mm) and electrode 2 is probably much closer to the task-relevant brain regions.

Potentially, the actual reason is a combination of both factors.

0.1 Hz to 8 Hz seems to be related to movement and other tasks in various brain areas. The results in Fig. 1 and 4 show that also the lowest frequency (in the literature, those bands are often denoted with delta (around 0 Hz to 4 Hz and theta (around 4 Hz to 8 Hz)) seem to be related with movement: the power slightly increases at `CueOn` (preparation period) and rises more strongly and abruptly at `ArmLift` or `ObjTouch`. However, as opposed to the mid-frequency (beta) decreased power, which was also present in

NOGO trials, low-frequency power is less pronounced or even decreased in NOGO trials.

In the literature, not many attention has been paid to lowest-frequency activity in the motor cortex using invasive EEG. In an MEG study (the authors claim that the MEG results are comparable to EEG), low-frequency (≤ 7 Hz) power increase was found in motor areas during movement [89]. Rickert et al. recorded increased low-frequency power in most of their motor cortical electrodes during a center-out movement when the movement started [88]. In the sensorimotor area, the theta band also becomes positive shortly after motion onset [90, 91] and motion offset [91] (though in [91] the effects are very weak). All these findings are in accord with the results of this work.

Looking at NOGO trials, low-frequency power rose only slightly at `CueOn` and went back to baseline level during the movement. This may suggest that it is involved in alertness (the thought that something has to be done soon) but not in the movement itself. In imagined movement, the low-frequency power even seems to decrease during the trial, similar to the beta power [82]. Other studies observed increased theta activity during virtual movement [92] in the neocortex and observed movement from a frontal view also lead to increased low-frequency power (Fig. 4 in this work) in the motor cortex. It is difficult to conclude what the role of lower frequencies in the motor cortex is, given the very different behaviors in conditions that lead to comparable results in other frequency ranges (as discussed above).

In the motor cortex, Waldert et al. could decode hand movement direction best with lowest-frequency power [89] and Jerbi et al. found a coupling between activity in lowest-frequency ranges and hand speed, so theta seems to be involved in geometrical and kinematic information of movements. In other brain areas, in particular in the hippocampus, theta oscillations were related to working memory [94–96], attention, surprise, and reaction to faults and punishment [97] (comparable to a power increase at `CueOn`) as well as virtual movement [92]. Delta oscillations were observed in the

cortex during sleep (e. g. [98]). As mentioned above, Ekstrom et al. also observed theta activity in the neocortex during virtual movement and they suggest that increased theta power helps bringing together different brain areas to execute a task [92]. Indeed, theta oscillation seems to be present throughout the brain during cognitive tasks [99].

Another question is why in the visual condition, the moment of low-frequency power increase differs with electrode depth. In the more superficial channels, it already rises at `ArmLift`, whereas in the deeper channels, it rises at `ObjTouch`, like in the motor responses. Very roughly speaking, more superficial layers in the neocortex are responsible for feedforward processes and processing sensory input, and deeper layers are responsible for feedback processes and comparing with previously learned “facts” [52]. A hypothesis could be that when we reach out to grasp an object, we mostly focus on the moment when we touch the object and not so much on the moment when we lift the arm and start the movement. When we observe an action, it is often the first movement that catches our attention. Getting back to the experiment, in visual trials, `ArmLift` is the event that caught the monkey’s attention, the most important input from the environment, whereas `ObjTouch` is the event that the monkey had remembered from the motor task, where `ObjTouch` was both the input from the environment and the “cue action” of the movement. Clearly, more evidence is needed to support this theory.

3.4.2 Summed-Up Power

As a next step, the sum of the power in certain time and frequency ranges of interest was taken and plotted against channels for each electrode and condition in order to compare the impact of electrode depth on the brain activity.

In the literature, not much work has been done on depth in the motor cortex. In general, feedforward pathways rather originate in the superficial cortical layers and feedback pathways rather originate in the deeper layers [52]. Now, there are two hypothesis that one could

make when comparing the results at different depths.

First, activity in superficial channels could be related with processing sensory input that is passed along to other brain areas (feedforward). In the same sense, activity in deeper channels could be associated with processes that profit from long-since-stored information (feedback).

Second, since feedforward processes have to react quickly, we could expect to have high powers at high frequencies in the more superficial channels and high powers at low frequencies in the deeper channels, because feedback signals are supposed to be more stable.

Considering only the motor responses for now, let’s first have a look at the mid-frequency range (15 Hz to 25 Hz). In superficial channels, the power is negative and goes towards baseline level with increasing depth, that is, that rather superficial layers are responsible for these oscillations. As we have discussed in Section 3.4.1, this frequency band is related to movement preparation because it also occurs in `NOGO` trials and already at `CueOn`. Therefore, preparing movement seems to be a feedforward process. On the other hand, the power in the high-frequency band (40 Hz to 60 Hz) is lower for more superficial channels and higher for the deepest channels. We associated this frequency band with the actual execution of actions. Using the same theory about cortical layers, this activity more seems to be related to feedback processes. Comparing with the first of the two hypotheses above, this makes sense: movement preparation is a reaction to sensory input, whereas the action execution is a learned behavior.

For the low-frequency range (0.1 Hz to 8 Hz), it is not so clear. Electrode 2 (which is presumably closer to the motor cortex) tends to have recorded higher powers in the more superficial channels during motion and the opposite during preparation. Thus, low-frequency activity during motion seems to be associated with a feedforward process which matches with the idea that this activity “connects” different brain areas to execute a task [92]. That electrode 3 sometimes has the opposite behavior may indicate that it was placed in an area that

is responsible for something else—or it is just an artifact.

Differences between motor and visual responses occur in the mid-frequency range, which is responsible for movement preparation. In the NOGO condition during the virtual movement period, the summed up power is weaker than in the GO condition for motor responses, but in both conditions there is a positive correlation, with the power close to baseline in the deepest channels. In the visual response however, the power is rather more negative in deeper layers than in more superficial layers. An explanation could be that the monkey was just paying less attention during NOGO trials, because it is obviously not very interesting to watch somebody doing nothing at all.

Nevertheless, the visual responses are quite similar in most cases, only that there are less significant correlations, that is, more noise. Generally speaking, this leads to the conclusion that when observing an action, the same processes are active—at different levels and at different points in time as the action enrolls. This property is crucial when it comes to really understanding or learning the action.

3.4.3 Statistically Relevant Distinction of Grip Types with Channel Depth

In general, the visual responses are bad predictors of grip types. In order to examine the previous observations with statistical tests, the “distinctions core” (see Materials and Methods, Section 3.2.3) was determined using Student’s t-test ($\alpha = 0.05$). The number of positive t-tests gives an indication of how well a frequency and time range might perform in predicting grip types from the power of the neuronal data.

Even though differences between the grip types could be identified by eye when looking at the averages across trials, given the high variance between the trials, the differences are not always significant, as Tables 3, 4, 5, and 6 show. The low-frequency range, which was identified as being responsible for the motion, its preparation and many underlying processes, apparently is the best frequency range to predict grip types from the motor responses. In

visual responses, high-frequency ranges (responsible for the motion itself) of electrode 3 seem to be doing even better. It was thought for electrode 3 that it was placed less close to the motor cortex than electrode 2.

These findings don’t look very promising when we attempt to predict grip types from mirror neuron activity in the motor cortex. A reason for this bad performance could be the high variance between the trials. This persuades the t-test to rate the grip types as being the same. Indeed, the NOGO trials had the tendency to have smaller variances (especially in the relevant time periods after motion onset) than GO trials, and according to the t-tests, the NOGO condition is in general a better predictor than the GO condition. Therefore, efforts have to be made to find a way to uniform the trials even more than just by removing the baseline.

Prediction ability depends on electrode depth in some cases. As a last step in the analysis, the Pearson correlation ($\alpha = 0.05$) of the distinction score with channel depth was determined.

In the low-frequency range, the motor GO trials (and NOGO trials in the movement preparation period) show a positive correlation between the distinction score and channel depth. This means that the deeper channels, the feedback processes, tend to have a better score. Apparently, the different movement types induce different low-frequency feedback processes in both the preparation and execution period of GO trials. When the movement is suppressed (NOGO trials), these processes no longer seem to be different for different grip types.

In the mid-frequency range, there are correlations in the NOGO trials only, almost always negative and, except for the time after CueOn, only for motor responses. A negative correlation means that the more superficial channels were better in distinguishing grip types. One could interpret this so that suppressing motion is more different in feedforward processes.

In the high-frequency ranges, almost no correlations can be seen. The few that are there are all in the NOGO condition. This is not surprising as we saw that in these frequencies, the distinction score was overall low.

4 Human SEEG

4.1 Background

Stereoencephalography (SEEG). The patients considered for this experiment suffer from a severe form of epilepsy that cannot be cured other than by surgery (see for instance Kahane et al., 2003 [100] or Tuxhorn et al., 2003 [101]). As part of the treatment, electrodes are implanted into their brains in order to identify epileptogenic zones (an epileptogenic zone is defined as “[t]he area of brain that is necessary and sufficient for initiating seizures and whose removal or disconnection is necessary for abolition of seizures” (Siegel, 2004 [102])).

Different recording methods allow to do this. Non-invasive methods like scalp electroencephalography (EEG) have the disadvantage that the signal is blocked by the skull, the skin, and other tissues due to their high resistance. Also, only if cortical activity is synchronized over areas of at least 6 cm^2 , it can be detected on the skull [103]. For a higher resolution and to detect smaller epileptic loci, recording sites have to be inside of the skull [104].

There are two types of intracranial electrodes: subdural grids (electrocorticography, ECoG) and depth electrodes (stereoencephalography, SEEG) and the choice depends on clinical need. Here, depth electrodes were used. They reduce the surgical trauma [105, 106] and penetrate the brain and can therefore also record from deeper brain areas [107], for instance from the hippocampus [108], the thalamus [109] or white matter [110]. However, no continuous areas in the cortex can be recorded [111]. Therefore, the placement of the electrodes has to be planned according to estimations based on non-invasive tests and is adapted to each patient individually [112, 113]. Nowadays, placements are assisted by surgical robots [114].

With SEEG, oscillatory activity in low-frequency as well as in gamma bands can be detected. As has been described in more detail in Section 2.2, power increases and decreases are among other things associated with motor tasks, so intracranial recordings provide precious data for analyzing mechanisms taking

place in the brain while executing or observing an action.

4.2 Materials and Methods

4.2.1 Data Collection

The data was collected from a patient suffering from intractable pharmaco-resistant epilepsy (aged 11, male) after obtaining informed consent from his parents. The patient had 17 stereoencephalography (SEEG) electrodes (with 4 to 16 channels each, PMT Corporation, Chanhassen, MN, USA) implanted for extended clinical monitoring and localization of seizure foci. The locations of the electrodes were determined by a robot and were entirely based on the requirements of the clinical evaluation. One electrode was placed in the frontal cortex. Only channels 8 to 15 on this electrode were considered in this work due to their proximity to the motor cortex.

4.2.2 Task

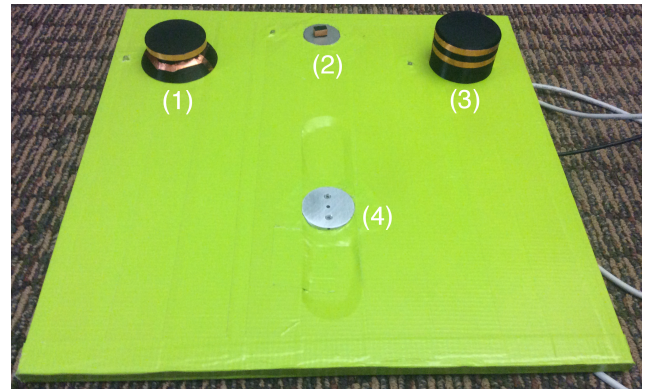


Figure 10: Picture of the board used for human experiments. (1) corresponds to prehension grip, (2) to precision grip, and (3) to power grip. (4) is the resting hand plate. For dimensions see text.

Measurements were taken using a tablet consisting of a $40.8\text{ cm} \times 40.8\text{ cm} \times 1.3\text{ cm}$ Plexiglas plate equipped with four touch sensors (AT42QT1011, SparkFun Electronics, Niwot, CO, USA), and three LED lights (Fig. 10). Three objects of different sizes and shapes were placed on the sensors. The touch sensors’ built in 10 nF capacitors (C2) were replaced with 1 nF capacitors in order to reduce the

sensitivity of the sensors, so that the mere placing of the objects is not enough to trigger a signal. The different shapes and sizes of the objects enforce the participants to perform specific grip types: power grip (1 in Fig. 10, a cylinder with diameter 6.35 cm and height 3.81 cm), precision grip (2, a rectangular plate with dimensions 0.76 cm \times 1.72 cm \times 0.76 cm), or prehension grip (3, a thin disk with diameter 5.54 cm and height 2.36 cm). The sensors and the lights were connected to the computer via a 12-bit data acquisition board (USB-1208FS, Measurement Computing Corporation, Norton, MA, USA) and controlled by custom scripts written in GNU Octave (version 4.1.0) using the Psychophysics toolbox [115].

The motor task was a GO/NOGO paradigm. The trial started when the participant placed their hand on the hand resting plate (4 on Fig. 10) and waited for the cue, which consisted of turning on the LED next to the selected object of the trial and lasted for 0.5 s (**CueOn**, this triggered a digital event and the time stamp at which the action occurred was stored for each trial). At the same time, a sound was played, lasting for 1.5 s to 4 s. In the case of a NOGO trial, the sound was white noise and the participant was not supposed to move but keep the hand on the hand resting plate for a total of 3 s to 4 s after the trial started. In the case of a GO trial, a “beep” sound (a pure tone of 1 kHz) was played. When the sound was stopped, the participant was allowed to start the movement (**GoSignal**). The next digital event was when the participant no longer touched the hand resting plate, reaching out for the object (**ArmLift**). Then the participant grasped the object (**ObjTouch**), released it (**ObjRelease**) and put the hand back to the hand resting plate (**HandBack**). All events after **GoSignal** were at the participant’s own pacing. The objects were selected in a pseudorandom order.

The tablet was placed on a bed table, in front of the patient who was brought to a semi-recumbent position in his hospital bed, so that he could comfortably reach all objects. During the execution of the motor tasks, the patient showed signs of difficulties with coordination as a consequence of the brain surgery he had

Visual	GO	NOGO
Prehension	16 to 18	21 to 23
Precision	17 to 20	15 to 18
Power	18 to 21	16 to 18

Table 7: Numbers of trials in the SEEG experiment with a human patient (only visual condition) that remained after removal of artifacts, depending on the channel.

to undergo just a few days before, so the motor task data was discarded and not used for further analysis. However, it allowed the patient to learn the task.

In the second part of the experiment, the patient was asked to observe the experimenter executing the task described above. The experimenter was sitting on the patient’s bedside, facing him at an angle of about 45° from frontal view, so that he could see the objects as well as the LED cues and the experimenter’s hand. The visual task was interrupted after roughly half of the trials and was, with agreement of the patient, taken up again with the remaining trials. The patient showed signs of tiredness and had to be reminded to keep focus from time to time.

4.2.3 Data Analysis

The data was collected in EDF (European Data Format) and converted to a Matlab file (Mathworks, Natick, MA, USA, version R2018b). Then, time-frequency spectra were obtained in the same way as described in Section 3.2.3. Only the electrode through the patient’s motor cortex was considered. The correctly executed trials from the two visual sessions were combined and kept for further analysis. The NOGO trials were aligned at **CueOn** and the GO trials at **ObjTouch**, and large time windows of 15 s and 7 s for NOGO trials and GO trials respectively were epoched. For both conditions and all three grip types, abnormally distributed trials and outliers (see Section 3.2.3) were discarded. The number of remaining trials was summarized in Table 7. Then, the multi-taper time-frequency spectrum was calculated using the Chronux toolbox [73] (5 tapers, time-bandwidth product of 4, window size of 0.75 s,

step size of 0.075 s) and converted to decibel. The baseline, defined as the time span from 600 ms to 100 ms before `CueOn`, was subtracted.

To check if the observed differences in the time-frequency analysis are statistically significant, the average power in three frequency ranges (0.1 Hz to 8 Hz, 10 Hz to 20 Hz, and 20 Hz to 30 Hz) and four time ranges (the 500 ms after `CueOn` and `GoSignal` and around `ObjTouch` and `ObjRelease`) was taken. For both conditions, the three combinations of grip pairs were compared using Student's t-test at $\alpha = 0.05$. For all grip types, GO and NOGO conditions were compared using Student's t-test at $\alpha = 0.05$ as well.

4.3 Results

In order to explore differences between species, the same experiment was run with a monkey and a human. Just as for the monkey, a multi-taper time-frequency analysis was computed for each condition and each grip type. Only the visual responses of the patient were used. Fig. 11 shows the modulation from the baseline (defined as 600 ms to 100 ms before `CueOn`) at six recording sites, where the most superficial one is on the top left. The vertical black lines correspond to the average time across trials (with standard deviation) of the events as the experiment enrolled. For GO trials, time $t = 0$ corresponds to `ObjTouch` and the events from left are `CueOn`, `GoSignal`, `ObjTouch`, `ObjRelease`, and `HandBack`. For NOGO trials, only `CueOn` is plotted ($t = 0$).

The differences between the grip types are quite notable in both GO trials and NOGO trials, though not all of them are of statistical significance. Table 8 summarizes the Student's t-significant differences in averaged powers in a certain frequency and time range at $\alpha = 0.05$. In NOGO trials, the grip types are only significantly different in upper channels after `ObjRelease`. Also in GO trials, the differences only become significant when the objects were touched. In the lower frequencies, the differences are more apparent in the lower channels, in the higher frequencies, there is only a difference in the most superficial channel of those studied. The mid-frequencies were the

same for all grip types, and apparently, only power could be distinguished from the others, but prehension and precision were the same.

Especially in the lower half of the channels, patches of positive power can be detected at all important events in GO power grips (after `CueOn`, at motion onset and offset) in a frequency range of about 20 Hz to 60 Hz (strongest between 20 Hz and 30 Hz). For GO precision trials, the activity in this band can only be detected after `CueOn`. For GO prehension, it's only at the end of the movement, when the hand released the object and went back to the resting plate. After `CueOn`, the power even becomes negative. However, a positive power patch can be observed in the NOGO trials at the time when `ObjTouch` would have taken place. A similar phenomenon can be detected in NOGO power trials and even (with some good will) in NOGO precision trials, but much weaker in these two grip types.

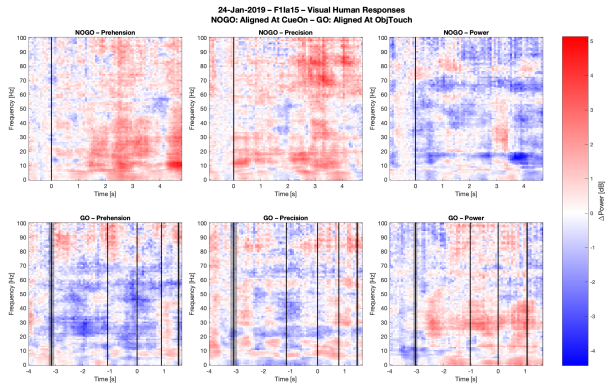
There is also activity in the lowest frequencies (about 0 Hz to 10 Hz) in GO power trials. For precision, it is interrupted at `ObjTouch` and for prehension, it is negative at almost all time. In NOGO trials, this band has a tendency to be more positive at most (virtual) events, except for power grips, where it is more negative.

Differences between GO and NOGO trials only become Student's t-significant ($\alpha = 0.05$) after motion onset. Table 9 summarizes all significant differences.

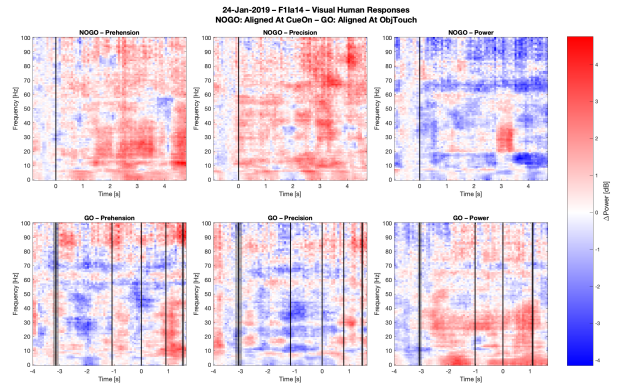
When comparing the human responses to the monkey visual responses (e. g. Fig. 7b), it is apparent that the blue beta band (negative power in 15 Hz to 25 Hz) is missing. It can only be guessed in some channels (e. g. Fig. 11a or 11f) for prehension grips in the GO condition. Generally speaking, more activity can be detected in the upper frequencies for the human responses than for the monkey's.

4.4 Discussion

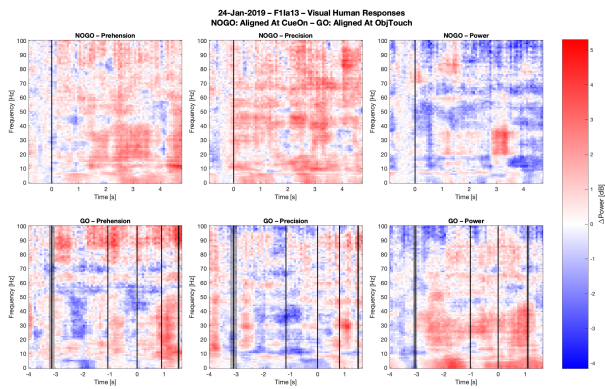
In the final part of this project, time-frequency power spectra in a cued GO/NOGO paradigm with a human (patient) were compared to the same experiment carried out with a monkey. In the monkey responses, there were several characteristic patterns in the following frequency



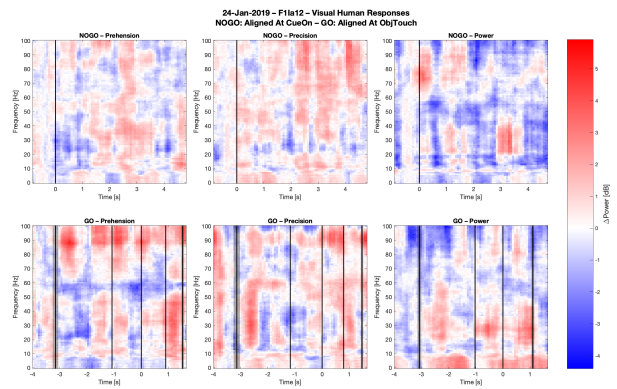
(a) Channel 15.



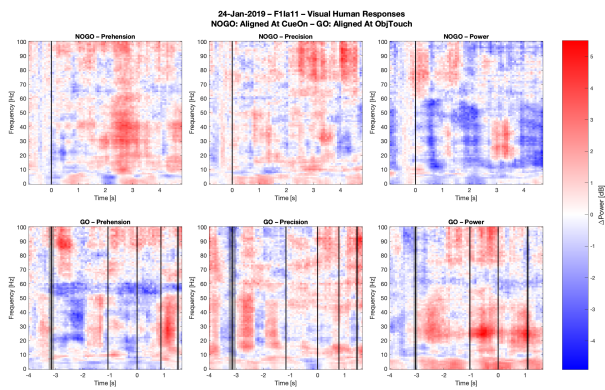
(b) Channel 14.



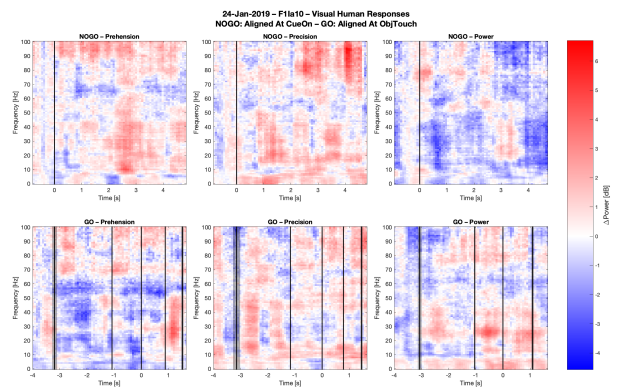
(c) Channel 13.



(d) Channel 12.



(e) Channel 11.



(f) Channel 10.

Figure 11: Time-frequency analyses of the human visual responses from the six electrodes of interest, GO and NOGO trials and the three grip types. Average of all trials. The plot on the top left (11a) corresponds to the most superficial channel, the plot on the bottom right (11f) to the deepest channel. NOGO trials were aligned with CueOn and GO trials were aligned with ObjTouch (time $t = 0$ s). The vertical black lines correspond to the average time of the occurrence of the events in the order: CueOn, GoSignal, ObjTouch, ObjRelease, HandBack, the black shade being the standard deviation. For NOGO trials, only CueOn is plotted.

Condition	Frequency	Aligned at	Time	Grip Comb.	Channels
GO	0.1 Hz to 8 Hz	ObjTouch	-250 ms to 250 ms	Preh-Pow	10, 11
GO	0.1 Hz to 8 Hz	ObjTouch	-250 ms to 250 ms	Prec-Pow	10, 11, 13
GO	0.1 Hz to 8 Hz	ObjRelease	-250 ms to 250 ms	Preh-Pow	12
GO	20 Hz to 30 Hz	ObjTouch	-250 ms to 250 ms	Preh-Pow	15
GO	20 Hz to 30 Hz	ObjTouch	-250 ms to 250 ms	Prec-Pow	15
NOGO	10 Hz to 20 Hz	ObjRelease	-250 ms to 250 ms	Preh-Pow	13, 14, 15
NOGO	10 Hz to 20 Hz	ObjRelease	-250 ms to 250 ms	Prec-Pow	13, 14, 15

Table 8: Student’s t-significant differences between grip type combinations ($\alpha = 0.05$). Preh: Prehension. Prec: Precision. Pow: Power.

Frequency	Aligned at	Time	Grip Type	Channels
0.1 Hz to 8 Hz	ObjTouch	-250 ms to 250 ms	Precision	13
0.1 Hz to 8 Hz	ObjTouch	-250 ms to 250 ms	Power	11
0.1 Hz to 8 Hz	ObjRelease	-250 ms to 250 ms	Power	11, 14
10 Hz to 20 Hz	GoSignal	0 ms to 500 ms	Precision	13, 14, 15
10 Hz to 20 Hz	ObjRelease	-250 ms to 250 ms	Power	11, 13, 14, 15
20 Hz to 30 Hz	GoSignal	0 ms to 500 ms	Prehension	15
20 Hz to 30 Hz	ObjTouch	-250 ms to 250 ms	Prehension	14, 15
20 Hz to 30 Hz	ObjRelease	-250 ms to 250 ms	Power	10, 11, 15

Table 9: Student’s t-significant differences between conditions ($\alpha = 0.05$).

ranges: low-frequency (0.1 Hz to 8 Hz), mid-frequency (15 Hz to 25 Hz), and high-frequency (40 Hz to 60 Hz).

For power grips, the power increased in the frequency band of 20 Hz to 40 Hz. This is similar to the monkey response, except that for the monkey, those “patches” didn’t already occur after CueOn, weren’t present in NOGO trials and occurred in a higher frequency range in NOGO trials. Also, in the other two grip types of the human responses, those power increases are only present after CueOn (precision grip) and after ObjRelease (prehension grip; to a less extent in precision grip). An increase in power at motion onset has already been observed in humans [33, 41, 86, 116, 117] but usually at higher frequencies (around 70 Hz to 100 Hz). Looking at the results here, there are also activities in the higher frequencies, but less specific to events for most conditions and channels. Also, those patches occur in NOGO trials as well, which was not the case for monkey responses, in the case of prehension even more than in NOGO trials. Possibly the patient could imagine the movements better even when they

were not executed, but of course it is difficult to draw conclusions from only one participant.

The power in the lowest frequency bands increases at some time points and decreases at others, depending on the condition and grip type. In the monkey responses, there was a tendency for increased power in GO trials and decreased power in NOGO trials. There were differences between the grip types but not to the extent of those in human responses. In Section 3.4.1, we discussed that these frequencies are associated with many different mechanisms in the brain. Possibly, when the patient was struggling to stay awake or distracted, many different processes were going on, and the differences between the grip types are not so much due to the different movements itself but to the different circumstances in each trial.

It is very interesting to notice that the negative power in the mid-frequency range, which was omnipresent in the monkey trials, is missing in the human trials. This frequency range has been associated with movement preparation and execution (see Section 3.4.1) and could also be seen in the monkey’s visual responses. It is unclear why this usually so prominent band

is missing. In the literature, several studies have shown this feature while human subjects executed a movement in non-invasive [116, 118] as well as in invasive [41, 86] measurements, so the negative beta band is not only present in monkeys. Not many studies however have been carried out with respect to action observation. Southgate et al. did an experiment where they compared the EEG responses of infants who had to grasp for objects and observe adults doing the same movement. In this case, the negative beta band was very prominent during the execution but not so much during the observation. Unlike the results of this work, the power never became positive [118].

Comparing the responses at different channels, that is, varying depth, it can be noticed that the patterns are in general consistent but are more focused in the intermediate channels (especially channels 11, Fig. 11e). This could indicate that the channels with the most focused responses were the closest to the motor cortex.

When looking at these results, one has to keep in mind that the data was recorded from only one, very young patient who was recovering from a brain surgery he had had two days before. His coordination ability was limited and he had to be reminded to keep focus as he was under the influence of medication. At the same time, visitors were sitting around his bed and there were many sources of distraction. Clearly, more data from patients have to be collected to exclude differences only due to different circumstances and to elaborate the actual differences between humans and monkeys more.

5 Conclusion

In this Master’s thesis, movement-specific characteristics of electrophysiological signals in a monkey motor area F5 during different grasping movements were identified. The characteristics of movement execution, movement preparation, and movement suppression were compared. Three frequency bands of special interest could be described: the movement itself seems to be encoded in 40 Hz to 60 Hz (often called “gamma band”), which results in positive power bursts when the fingers are moved. The preparation

of the movement and the execution could be observed in 15 Hz to 25 Hz (the “beta band”) as negative power in GO and NOGO conditions. In the lowest frequencies up to 8 Hz (“delta/theta band”), event-related power modulations occur. All of these characteristics occur not only in the motor responses but also in the visual responses, even the power modulations in the higher frequencies which were absent in NOGO trials. This implies that observing an action activates the same processes in the monkey motor cortex as executing it. The visual responses to the different grip types however were only significantly different in rare cases. This does nevertheless not mean that the intermediate goal of an observed action is not encoded in motor area F5, but that ways have to be found in order to reduce the variability between trials in the same condition.

Thanks to the electrodes that were used for the LFP recordings, which allowed to measure simultaneously at different sites, brain activity in the cortex could also be studied with regard to depth. With increasing depth, activity (positive or negative power) increased for processes related to feedback mechanisms and decreased for processes related to feedforward mechanisms. This approach provides an interesting field to study the function of different cortical layers.

In a second part, the same experiment was run with a patient of the Boston Children’s Hospital. Even though the analysis was difficult due to the patient’s condition during the experiment, at least in the power grip the same high-frequency characteristics could be detected in the visual responses, even though it occurred earlier and in lower frequencies. Also, the beta band power decrease was missing in all conditions and the activity of the lowest frequencies was inconsistent between conditions. This could not be explained with the literature.

Therefore, more data has to be collected from humans in order to conclude if these differences are an exception or if there is a trend specific to this task.

This project gave a first insight in action decoding of visual responses. In the future, algorithms to precisely decode actions from visual responses could become very promising in

the field of brain machine interfaces and robot control by action observation. In addition to that, it can give insight into how we understand each other in social interactions. In this manner, new ways to treat disorders that affect communication skills (e. g. autism) could be developed.

Also, a first step was taken for the direct comparison between monkeys and humans. The experimental equipment was finalized and we are ready to continue measurements with patients. The first available data show that more subjects are needed to draw valid conclusions in order to answer the question if and in which cases monkeys serve as a good model for humans, and which brain areas serve as homologues.

References

- [1] Richard Cook et al. “Mirror neurons: From origin to function”. In: *Behavioral and Brain Sciences* 37.2 (Apr. 2014), pp. 177–192. ISSN: 0140-525X, 1469-1825. DOI: 10.1017/S0140525X13000903. URL: <https://www.cambridge.org/core/journals/behavioral-and-brain-sciences/article/mirror-neurons-from-origin-to-function/A376CF4E7269CADFCD9D563A39ADED0> (visited on 02/04/2019).
- [2] Antonino Casile, Vittorio Caggiano, and Pier Francesco Ferrari. “The Mirror Neuron System: A Fresh View”. In: *The Neuroscientist* 17.5 (Oct. 1, 2011), pp. 524–538. ISSN: 1073-8584. DOI: 10.1177/1073858410392239. URL: <https://doi.org/10.1177/1073858410392239> (visited on 08/15/2018).
- [3] G. di Pellegrino et al. “Understanding motor events: a neurophysiological study”. In: *Experimental Brain Research* 91.1 (Oct. 1, 1992), pp. 176–180. ISSN: 0014-4819, 1432-1106. DOI: 10.1007/BF00230027. URL: <https://link.springer.com/article/10.1007/BF00230027> (visited on 08/16/2018).
- [4] Vittorio Gallese et al. “Action recognition in the premotor cortex. *Brain* 119, 593-609”. In: *Brain : a journal of neurology* 119 (Pt 2) (May 1, 1996), pp. 593–609. DOI: 10.1093/brain/119.2.593.
- [5] G. Rizzolatti et al. “Premotor cortex and the recognition of motor actions”. In: *Brain Research. Cognitive Brain Research* 3.2 (Mar. 1996), pp. 131–141. ISSN: 0926-6410.
- [6] Vittorio Caggiano et al. “Encoding of point of view during action observation in the local field potentials of macaque area F5”. In: *European Journal of Neuroscience* 41.4 (2015), pp. 466–476. ISSN: 1460-9568. DOI: 10.1111/ejn.12793. URL: <https://onlinelibrary.wiley.com/doi/abs/10.1111/ejn.12793> (visited on 01/22/2019).
- [7] Giacomo Rizzolatti and Laila Craighero. “The mirror-neuron system”. In: *Annual Review of Neuroscience* 27 (2004), pp. 169–192. ISSN: 0147-006X. DOI: 10.1146/annurev.neuro.27.070203.144230.
- [8] Lynn T. Kozlowski and James E. Cutting. “Recognizing the sex of a walker from a dynamic point-light display”. In: *Perception & Psychophysics* 21.6 (Nov. 1, 1977), pp. 575–580. ISSN: 0031-5117, 1532-5962. DOI: 10.3758/BF03198740. URL: <https://link.springer.com/article/10.3758/BF03198740> (visited on 08/14/2018).
- [9] Gunnar Johansson. “Visual perception of biological motion and a model for its analysis”. In: *Perception & Psychophysics* 14.2 (June 1, 1973), pp. 201–211. ISSN: 0031-5117, 1532-5962. DOI: 10.3758/BF03212378. URL: <https://link.springer.com/article/10.3758/BF03212378> (visited on 08/14/2018).
- [10] Cristina Becchio et al. “Both your intention and mine are reflected in the kinematics of my reach-to-grasp movement”. In: *Cognition* 106.2 (Feb. 2008), pp. 894–912. ISSN: 0010-0277. DOI: 10.1016/j.cognition.2007.05.004.

- [11] Cristina Becchio et al. “The case of Dr. Jekyll and Mr. Hyde: A kinematic study on social intention”. In: *Consciousness and Cognition* 17.3 (Sept. 1, 2008), pp. 557–564. ISSN: 1053-8100. DOI: 10.1016/j.concog.2007.03.003. URL: <http://www.sciencedirect.com/science/article/pii/S1053810007000207> (visited on 08/14/2018).
- [12] Winand H Dittrich et al. “Perception of Emotion from Dynamic Point-Light Displays Represented in Dance”. In: *Perception* 25.6 (June 1, 1996), pp. 727–738. ISSN: 0301-0066. DOI: 10.1068/p250727. URL: <https://doi.org/10.1068/p250727> (visited on 08/14/2018).
- [13] Nick Barraclough et al. “Visual Adaptation to Goal-directed Hand Actions”. In: *Journal of cognitive neuroscience* 21 (Nov. 1, 2008), pp. 1806–20. DOI: 10.1162/jocn.2008.21145.
- [14] Robert W. Mitchell. “A Comparative-Developmental Approach to Understanding Imitation”. en. In: *Perspectives in Ethology: Volume 7 Alternatives*. Ed. by P. P. G. Bateson and Peter H. Klopfer. Boston, MA: Springer US, 1987, pp. 183–215. ISBN: 978-1-4613-1815-6. DOI: 10.1007/978-1-4613-1815-6_7. URL: https://doi.org/10.1007/978-1-4613-1815-6_7 (visited on 01/31/2019).
- [15] Thomas R. Zentall. “Imitation by Animals: How Do They Do It?” en. In: *Current Directions in Psychological Science* 12.3 (June 2003), pp. 91–95. ISSN: 0963-7214. DOI: 10.1111/1467-8721.01237. URL: <https://doi.org/10.1111/1467-8721.01237> (visited on 01/31/2019).
- [16] Giacomo Rizzolatti, Leonardo Fogassi, and Vittorio Gallese. *Neurophysiological Mechanisms Underlying the Understanding and Imitation of Action*. Vol. 2. Oct. 1, 2001. 661 pp. DOI: 10.1038/35090060.
- [17] Evelyne Kohler et al. “Hearing Sounds, Understanding Actions: Action Representation in Mirror Neurons”. en. In: *Science* 297.5582 (Aug. 2002), pp. 846–848. ISSN: 0036-8075, 1095-9203. DOI: 10.1126/science.1070311. URL: <http://science.sciencemag.org/content/297/5582/846> (visited on 01/31/2019).
- [18] Henri J Gastaut and Jacques Bert. “EEG changes during cinematographic presentation (Moving picture activation of the EEG)”. In: *Electroencephalography and Clinical Neurophysiology* 6 (Jan. 1954), pp. 433–444. ISSN: 0013-4694. DOI: 10.1016/0013-4694(54)90058-9. URL: <http://www.sciencedirect.com/science/article/pii/0013469454900589> (visited on 01/31/2019).
- [19] L. Fadiga et al. “Motor facilitation during action observation: a magnetic stimulation study”. In: *Journal of Neurophysiology* 73.6 (June 1995), pp. 2608–2611. ISSN: 0022-3077. DOI: 10.1152/jn.1995.73.6.2608.
- [20] Fumiko Maeda, Galit Kleiner-fisman, and Alvaro Pascual-leone. “Motor facilitation while observing hand actions: Specificity of the effect and role of observer’s orientation”. In: *J. Neurophysiol* (2002), pp. 1329–1335.
- [21] Simone Patuzzo, Antonio Fiaschi, and Paolo Manganotti. “Modulation of motor cortex excitability in the left hemisphere during action observation: a single- and paired-pulse transcranial magnetic stimulation study of self- and non-self-action observation”. In: *Neuropsychologia* 41.9 (2003), pp. 1272–1278. ISSN: 0028-3932.
- [22] D. Huberdeau et al. “Analysis of local field potential signals: A systems approach”. In: *2011 Annual International Conference of the IEEE Engineering in Medicine and Biology Society*. 2011 Annual International Conference of the IEEE Engineering in Medicine and Biology Society. Aug. 2011, pp. 814–817. DOI: 10.1109/IEMBS.2011.6090186.

- [23] Alberto Mazzoni, Nikos K. Logothetis, and Stefano Panzeri. “The information content of Local Field Potentials: experiments and models”. In: (June 4, 2012). URL: <https://arxiv.org/abs/1206.0560?context=q-bio.NC> (visited on 10/02/2018).
- [24] David P. Nguyen et al. “Measuring instantaneous frequency of local field potential oscillations using the Kalman smoother”. In: *Journal of Neuroscience Methods* 184.2 (Nov. 15, 2009), pp. 365–374. ISSN: 0165-0270. DOI: 10.1016/j.jneumeth.2009.08.012. URL: <http://www.sciencedirect.com/science/article/pii/S0165027009004427> (visited on 10/02/2018).
- [25] Hans Berger. “Das Elektrenkephalogramm des Menschen”. In: *Naturwissenschaften* 23.8 (Feb. 1, 1935), pp. 121–124. ISSN: 1432-1904. DOI: 10.1007/BF01496966. URL: <https://doi.org/10.1007/BF01496966> (visited on 10/03/2018).
- [26] Yoshinao Kajikawa and Charles E. Schroeder. “How Local Is the Local Field Potential?” In: *Neuron* 72.5 (Dec. 8, 2011), pp. 847–858. ISSN: 0896-6273. DOI: 10.1016/j.neuron.2011.09.029. URL: <http://www.sciencedirect.com/science/article/pii/S089662731100883X> (visited on 09/27/2018).
- [27] M. Steriade and J.A. Hobson. “Neuronal activity during the sleep-waking cycle”. In: *Progress in Neurobiology* 6 (1976), pp. 157–376. ISSN: 03010082. DOI: 10.1016/0301-0082(76)90013-7. URL: <http://linkinghub.elsevier.com/retrieve/pii/0301008276900137> (visited on 10/03/2018).
- [28] Mircea Steriade. “Alertness, Quiet Sleep, Dreaming”. In: *Normal and Altered States of Function*. Ed. by Alan Peters and Edward G. Jones. Red. by Edward G. Jones and Alan Peters. Vol. 9. Boston, MA: Springer US, 1991, pp. 279–357. ISBN: 978-1-4615-6624-3 978-1-4615-6622-9. DOI: 10.1007/978-1-4615-6622-9_8. URL: http://link.springer.com/10.1007/978-1-4615-6622-9_8 (visited on 10/03/2018).
- [29] Nikos K. Logothetis. “The Underpinnings of the BOLD Functional Magnetic Resonance Imaging Signal”. In: *The Journal of Neuroscience* 23.10 (May 15, 2003), pp. 3963–3971. ISSN: 0270-6474, 1529-2401. DOI: 10.1523/JNEUROSCI.23-10-03963.2003. URL: <http://www.jneurosci.org/lookup/doi/10.1523/JNEUROSCI.23-10-03963.2003> (visited on 10/03/2018).
- [30] Andrei Belitski et al. “Low-Frequency Local Field Potentials and Spikes in Primary Visual Cortex Convey Independent Visual Information”. In: *Journal of Neuroscience* 28.22 (May 28, 2008), pp. 5696–5709. ISSN: 0270-6474, 1529-2401. DOI: 10.1523/JNEUROSCI.0009-08.2008. URL: <http://www.jneurosci.org/content/28/22/5696> (visited on 10/03/2018).
- [31] Tonio Ball et al. “Movement related activity in the high gamma range of the human EEG”. In: *NeuroImage* 41.2 (June 1, 2008), pp. 302–310. ISSN: 1053-8119. DOI: 10.1016/j.neuroimage.2008.02.032. URL: <http://www.sciencedirect.com/science/article/pii/S1053811908001717> (visited on 10/05/2018).
- [32] Jan-Mathijs Schoffelen, Robert Oostenveld, and Pascal Fries. “Neuronal Coherence as a Mechanism of Effective Corticospinal Interaction”. In: *Science* 308.5718 (Apr. 1, 2005), pp. 111–113. ISSN: 0036-8075, 1095-9203. DOI: 10.1126/science.1107027. URL: <http://science.sciencemag.org/content/308/5718/111> (visited on 10/05/2018).
- [33] N. E. Crone et al. “Functional mapping of human sensorimotor cortex with electrocorticographic spectral analysis. I. Alpha and beta event-related desynchronization.” In: *Brain* 121.12 (Dec. 1, 1998), pp. 2271–2299. ISSN: 0006-8950. DOI: 10.1093/brain/121.12.2271. URL: <https://academic.oup.com/>

- brain/article/121/12/2271/371495 (visited on 01/28/2019).
- [34] Douglas Cheyne et al. “Self-paced movements induce high-frequency gamma oscillations in primary motor cortex”. In: *NeuroImage* 42.1 (Aug. 1, 2008), pp. 332–342. ISSN: 1053-8119. DOI: 10.1016/j.neuroimage.2008.04.178. URL: <http://www.sciencedirect.com/science/article/pii/S1053811908004965> (visited on 10/05/2018).
- [35] Soumyadipta Acharya et al. “Electrocorticographic amplitude predicts finger positions during slow grasping motions of the hand”. In: *Journal of neural engineering* 7.4 (Aug. 2010), p. 046002. ISSN: 1741-2560. DOI: 10.1088/1741-2560/7/4/046002. URL: <https://www.ncbi.nlm.nih.gov/pmc/articles/PMC4021582/> (visited on 10/09/2018).
- [36] J. Kubánek et al. “Decoding Flexion of Individual Fingers Using Electrocorticographic Signals in Humans”. In: *Journal of neural engineering* 6.6 (Dec. 2009), p. 066001. ISSN: 1741-2560. DOI: 10.1088/1741-2560/6/6/066001. URL: <https://www.ncbi.nlm.nih.gov/pmc/articles/PMC3664231/> (visited on 10/09/2018).
- [37] K. J. Miller et al. “Decoupling the Cortical Power Spectrum Reveals Real-Time Representation of Individual Finger Movements in Humans”. In: *Journal of Neuroscience* 29.10 (Mar. 11, 2009), pp. 3132–3137. ISSN: 0270-6474, 1529-2401. DOI: 10.1523/JNEUROSCI.5506-08.2009. URL: <http://www.jneurosci.org/content/29/10/3132> (visited on 10/09/2018).
- [38] Tobias Pistohl et al. “Prediction of arm movement trajectories from ECoG-recordings in humans”. In: *Journal of Neuroscience Methods* 167.1 (Jan. 2008), pp. 105–114. ISSN: 01650270. DOI: 10.1016/j.jneumeth.2007.10.001. URL: <http://linkinghub.elsevier.com/retrieve/pii/S0165027007004840> (visited on 10/09/2018).
- [39] G. Schalk et al. “Decoding two-dimensional movement trajectories using electrocorticographic signals in humans”. In: *Journal of Neural Engineering* 4.3 (Sept. 2007), pp. 264–275. ISSN: 1741-2560. DOI: 10.1088/1741-2560/4/3/012.
- [40] Eric C. Leuthardt et al. “A brain–computer interface using electrocorticographic signals in humans”. In: *Journal of Neural Engineering* 1.2 (2004), p. 63. ISSN: 1741-2552. DOI: 10.1088/1741-2560/1/2/001. URL: <http://stacks.iop.org/1741-2552/1/i=2/a=001> (visited on 10/09/2018).
- [41] G. Pfurtscheller et al. “Spatiotemporal patterns of beta desynchronization and gamma synchronization in corticographic data during self-paced movement”. In: *Clinical Neurophysiology* 114.7 (July 1, 2003), pp. 1226–1236. ISSN: 1388-2457. DOI: 10.1016/S1388-2457(03)00067-1. URL: <http://www.sciencedirect.com/science/article/pii/S1388245703000671> (visited on 10/12/2018).
- [42] G Pfurtscheller and R Cooper. “Frequency dependence of the transmission of the EEG from cortex to scalp”. In: *Electroencephalography and Clinical Neurophysiology* 38.1 (Jan. 1, 1975), pp. 93–96. ISSN: 0013-4694. DOI: 10.1016/0013-4694(75)90215-1. URL: <http://www.sciencedirect.com/science/article/pii/0013469475902151> (visited on 10/09/2018).
- [43] Jean-Philippe Lachaux et al. “The many faces of the gamma band response to complex visual stimuli”. In: *NeuroImage* 25.2 (Apr. 1, 2005), pp. 491–501. ISSN: 1053-8119. DOI: 10.1016/j.neuroimage.2004.11.052. URL: <http://www.sciencedirect.com/science/article/pii/S1053811904007347> (visited on 10/12/2018).
- [44] Shinji Ohara et al. “Movement-related change of electrocorticographic activity in human supplementary motor area proper”. In: *Brain* 123.6 (June 1, 2000), pp. 1203–1215. ISSN: 0006-8950. DOI:

- 10.1093/brain/123.6.1203. URL: <https://academic.oup.com/brain/article/123/6/1203/441943> (visited on 10/15/2018).
- [45] Michael J Kahana, David Seelig, and Joseph R Madsen. “Theta returns”. In: *Current Opinion in Neurobiology* 11.6 (Dec. 1, 2001), pp. 739–744. ISSN: 0959-4388. DOI: 10.1016/S0959-4388(01)00278-1. URL: <http://www.sciencedirect.com/science/article/pii/S0959438801002781> (visited on 10/15/2018).
- [46] Ole Jensen and Laura L. Colgin. “Cross-frequency coupling between neuronal oscillations”. In: *Trends in Cognitive Sciences* 11.7 (July 2007), pp. 267–269. ISSN: 1364-6613. DOI: 10.1016/j.tics.2007.05.003.
- [47] Ryan T. Canolty and Robert T. Knight. “The functional role of cross-frequency coupling”. In: *Trends in Cognitive Sciences* 14.11 (Nov. 2010), pp. 506–515. ISSN: 1364-6613. DOI: 10.1016/j.tics.2010.09.001. URL: <https://www.ncbi.nlm.nih.gov/pmc/articles/PMC3359652/> (visited on 10/11/2018).
- [48] R. T. Canolty et al. “High Gamma Power Is Phase-Locked to Theta Oscillations in Human Neocortex”. In: *Science (New York, N.Y.)* 313.5793 (Sept. 15, 2006), pp. 1626–1628. ISSN: 0036-8075. DOI: 10.1126/science.1128115. URL: <https://www.ncbi.nlm.nih.gov/pmc/articles/PMC2628289/> (visited on 10/11/2018).
- [49] Kai J. Miller et al. “Dynamic Modulation of Local Population Activity by Rhythm Phase in Human Occipital Cortex During a Visual Search Task”. In: *Frontiers in Human Neuroscience* 4 (2010). ISSN: 1662-5161. DOI: 10.3389/fnhum.2010.00197. URL: <https://www.frontiersin.org/articles/10.3389/fnhum.2010.00197/full> (visited on 10/11/2018).
- [50] Biyu J. He et al. “The temporal structures and functional significance of scale-free brain activity”. In: *Neuron* 66.3 (May 13, 2010), pp. 353–369. ISSN: 0896-6273. DOI: 10.1016/j.neuron.2010.04.020. URL: <https://www.ncbi.nlm.nih.gov/pmc/articles/PMC2878725/> (visited on 10/11/2018).
- [51] Simona Lodato and Paola Arlotta. “Generating Neuronal Diversity in the Mammalian Cerebral Cortex”. In: *Annual Review of Cell and Developmental Biology* 31.1 (Nov. 13, 2015), pp. 699–720. ISSN: 1081-0706. DOI: 10.1146/annurev-cellbio-100814-125353. URL: <https://www.annualreviews.org/doi/10.1146/annurev-cellbio-100814-125353> (visited on 01/28/2019).
- [52] Nikola T Markov and Henry Kennedy. “The importance of being hierarchical”. In: *Current Opinion in Neurobiology*. Macrocircuits 23.2 (Apr. 1, 2013), pp. 187–194. ISSN: 0959-4388. DOI: 10.1016/j.conb.2012.12.008. URL: <http://www.sciencedirect.com/science/article/pii/S0959438813000123> (visited on 01/28/2019).
- [53] D. Mumford. “On the computational architecture of the neocortex - II The role of cortico-cortical loops”. In: *Biological Cybernetics* 66.3 (1992), pp. 241–251. DOI: 10.1007/BF00198477.
- [54] A. Clark. “Whatever next? Predictive brains, situated agents, and the future of cognitive science”. In: *Behavioral and Brain Sciences* 36.3 (2013), pp. 181–204. DOI: 10.1017/S0140525X12000477.
- [55] Hae-Jeong Park and Karl Friston. “Structural and Functional Brain Networks: From Connections to Cognition”. In: *Science* 342.6158 (Nov. 1, 2013), p. 1238411. ISSN: 0036-8075, 1095-9203. DOI: 10.1126/science.1238411. URL: <http://science.sciencemag.org/content/342/6158/1238411> (visited on 01/28/2019).

- [56] T.S. Lee and D. Mumford. “Hierarchical Bayesian inference in the visual cortex”. In: *Journal of the Optical Society of America A: Optics and Image Science, and Vision* 20.7 (2003), pp. 1434–1448. DOI: 10.1364/JOSAA.20.001434.
- [57] Charles D. Gilbert and Mariano Sigman. “Brain States: Top-Down Influences in Sensory Processing”. In: *Neuron* 54.5 (June 7, 2007), pp. 677–696. ISSN: 0896-6273. DOI: 10.1016/j.neuron.2007.05.019. URL: <http://www.sciencedirect.com/science/article/pii/S0896627307003765> (visited on 01/28/2019).
- [58] André Moraes Bastos et al. “Visual Areas Exert Feedforward and Feedback Influences through Distinct Frequency Channels”. In: *Neuron* 85.2 (Jan. 21, 2015), pp. 390–401. ISSN: 0896-6273. DOI: 10.1016/j.neuron.2014.12.018. URL: <http://www.sciencedirect.com/science/article/pii/S089662731401099X> (visited on 01/28/2019).
- [59] T. Van Kerkoerle et al. “Alpha and gamma oscillations characterize feedback and feedforward processing in monkey visual cortex”. In: *Proceedings of the National Academy of Sciences of the United States of America* 111.40 (2014), pp. 14332–14341. DOI: 10.1073/pnas.1402773111.
- [60] O. Maier and C.M. Wiethoff. “N-terminal-helix-independent membrane interactions facilitate adenovirus protein VI induction of membrane tubule formation”. In: *Virology* 408.1 (2010), pp. 31–38. DOI: 10.1016/j.virol.2010.08.033.
- [61] E.A. Buffalo et al. “Laminar differences in gamma and alpha coherence in the ventral stream”. In: *Proceedings of the National Academy of Sciences of the United States of America* 108.27 (2011), pp. 11262–11267. DOI: 10.1073/pnas.1011284108.
- [62] A.K. Roopun et al. “A beta2-frequency (20-30 Hz) oscillation in nonsynaptic networks of somatosensory cortex”. In: *Proceedings of the National Academy of Sciences of the United States of America* 103.42 (2006), pp. 15646–15650. DOI: 10.1073/pnas.0607443103.
- [63] Anita K. Roopun et al. “Period concatenation underlies interactions between gamma and beta rhythms in neocortex”. In: *Frontiers in Cellular Neuroscience* 2 (2008). ISSN: 1662-5102. DOI: 10.3389/neuro.03.001.2008. URL: <https://www.frontiersin.org/articles/10.3389/neuro.03.001.2008/full> (visited on 01/28/2019).
- [64] Andre M. Bastos et al. “Canonical Microcircuits for Predictive Coding”. In: *Neuron* 76.4 (Nov. 21, 2012), pp. 695–711. ISSN: 0896-6273. DOI: 10.1016/j.neuron.2012.10.038. URL: <http://www.sciencedirect.com/science/article/pii/S0896627312009592> (visited on 01/28/2019).
- [65] György Buzsáki, Costas A. Anastassiou, and Christof Koch. “The origin of extracellular fields and currents — EEG, ECoG, LFP and spikes”. In: *Nature Reviews Neuroscience* 13.6 (June 2012), pp. 407–420. ISSN: 1471-0048. DOI: 10.1038/nrn3241. URL: <https://www.nature.com/articles/nrn3241> (visited on 09/25/2018).
- [66] Nikos K. Logothetis, Christoph Kayser, and Axel Oeltermann. “In Vivo Measurement of Cortical Impedance Spectrum in Monkeys: Implications for Signal Propagation”. In: *Neuron* 55.5 (Sept. 6, 2007), pp. 809–823. ISSN: 0896-6273. DOI: 10.1016/j.neuron.2007.07.027. URL: <http://www.sciencedirect.com/science/article/pii/S0896627307005727> (visited on 09/27/2018).
- [67] Virginie Briffaud et al. “The Relationship between Respiration-Related Membrane Potential Slow Oscillations and Discharge Patterns in Mitral/Tufted Cells: What Are the Rules?” In: *PLOS ONE* 7.8 (Aug. 31, 2012), e43964. ISSN:

- 1932-6203. DOI: 10.1371/journal.pone.0043964. URL: <https://journals.plos.org/plosone/article?id=10.1371/journal.pone.0043964> (visited on 10/02/2018).
- [68] Bijan Pesaran et al. “Temporal structure in neuronal activity during working memory in macaque parietal cortex”. In: *Nature Neuroscience* 5.8 (Aug. 2002), pp. 805–811. ISSN: 1546-1726. DOI: 10.1038/nn890. URL: <https://www.nature.com/articles/nn890> (visited on 10/02/2018).
- [69] Carsten Mehring et al. “Inference of hand movements from local field potentials in monkey motor cortex”. In: *Nature neuroscience* 6 (Jan. 1, 2004), pp. 1253–4. DOI: 10.1038/nn1158.
- [70] Malte J. Rasch et al. “Inferring Spike Trains From Local Field Potentials”. In: *Journal of Neurophysiology* 99.3 (Mar. 1, 2008), pp. 1461–1476. ISSN: 0022-3077. DOI: 10.1152/jn.00919.2007. URL: <https://www.physiology.org/doi/full/10.1152/jn.00919.2007> (visited on 10/02/2018).
- [71] Bijan Pesaran. “Uncovering the Mysterious Origins of Local Field Potentials”. In: *Neuron* 61.1 (Jan. 15, 2009), pp. 1–2. ISSN: 0896-6273. DOI: 10.1016/j.neuron.2008.12.019. URL: <http://www.sciencedirect.com/science/article/pii/S089662730801091X> (visited on 09/27/2018).
- [72] Monica Maranesi et al. “Monkey gaze behaviour during action observation and its relationship to mirror neuron activity”. In: *The European Journal of Neuroscience* 38.12 (Dec. 2013), pp. 3721–3730. ISSN: 1460-9568. DOI: 10.1111/ejn.12376.
- [73] Hemant Bokil et al. “Chronux: a platform for analyzing neural signals”. In: *Journal of Neuroscience Methods* 192.1 (Sept. 30, 2010), pp. 146–151. ISSN: 1872-678X. DOI: 10.1016/j.jneumeth.2010.06.020.
- [74] Herbert Jasper and Wilder Penfield. “Electrocorticograms in man: Effect of voluntary movement upon the electrical activity of the precentral gyrus”. In: *Archiv für Psychiatrie und Nervenkrankheiten* 183.1 (Jan. 1, 1949), pp. 163–174. ISSN: 1433-8491. DOI: 10.1007/BF01062488. URL: <https://doi.org/10.1007/BF01062488> (visited on 01/26/2019).
- [75] Preeya Khanna and Jose M Carmena. “Beta band oscillations in motor cortex reflect neural population signals that delay movement onset”. In: *eLife* 6 (). ISSN: 2050-084X. DOI: 10.7554/eLife.24573. URL: <https://www.ncbi.nlm.nih.gov/pmc/articles/PMC5468088/> (visited on 01/27/2019).
- [76] C. Tzagarakis et al. “Beta-Band Activity during Motor Planning Reflects Response Uncertainty”. In: *Journal of Neuroscience* 30.34 (Aug. 25, 2010), pp. 11270–11277. ISSN: 0270-6474, 1529-2401. DOI: 10.1523/JNEUROSCI.6026-09.2010. URL: <http://www.jneurosci.org/cgi/doi/10.1523/JNEUROSCI.6026-09.2010> (visited on 01/26/2019).
- [77] Andrea A. Kühn et al. “Event-related beta desynchronization in human subthalamic nucleus correlates with motor performance”. In: *Brain* 127.4 (Apr. 1, 2004), pp. 735–746. ISSN: 0006-8950. DOI: 10.1093/brain/awh106. URL: <https://academic.oup.com/brain/article/127/4/735/398200> (visited on 01/26/2019).
- [78] Malcolm Proudfoot et al. “Altered cortical beta-band oscillations reflect motor system degeneration in amyotrophic lateral sclerosis”. In: *Human Brain Mapping* 38.1 (2017), pp. 237–254. ISSN: 1097-0193. DOI: 10.1002/hbm.23357. URL: <https://onlinelibrary.wiley.com/doi/abs/10.1002/hbm.23357> (visited on 01/27/2019).
- [79] G. Pfurtscheller and F. H. Lopes da Silva. “Event-related EEG/MEG synchronization and desynchronization: basic principles”. In: *Clinical Neurophysiol-*

- ogy 110.11 (Nov. 1, 1999), pp. 1842–1857. ISSN: 1388-2457. DOI: 10.1016/S1388-2457(99)00141-8. URL: <http://www.sciencedirect.com/science/article/pii/S1388245799001418> (visited on 01/26/2019).
- [80] Nicole Swann et al. “Intracranial EEG reveals a time- and frequency-specific role for the right inferior frontal gyrus and primary motor cortex in stopping initiated responses”. In: *The Journal of Neuroscience : the official journal of the Society for Neuroscience* 29.40 (Oct. 7, 2009), pp. 12675–12685. ISSN: 0270-6474. DOI: 10.1523/JNEUROSCI.3359-09.2009. URL: <https://www.ncbi.nlm.nih.gov/pmc/articles/PMC2801605/> (visited on 01/26/2019).
- [81] Y. Zhang et al. “Response preparation and inhibition: The role of the cortical sensorimotor beta rhythm”. In: *Neuroscience* 156.1 (Sept. 22, 2008), pp. 238–246. ISSN: 0306-4522. DOI: 10.1016/j.neuroscience.2008.06.061. URL: <http://www.sciencedirect.com/science/article/pii/S0306452208009809> (visited on 01/26/2019).
- [82] Floris P. de Lange et al. “Interactions Between Posterior Gamma and Frontal Alpha/Beta Oscillations During Imagined Actions”. In: *Frontiers in Human Neuroscience* 2 (Aug. 20, 2008). ISSN: 1662-5161. DOI: 10.3389/neuro.09.007.2008. URL: <https://www.ncbi.nlm.nih.gov/pmc/articles/PMC2572199/> (visited on 01/26/2019).
- [83] D. M. Wegner and S. Zanakos. “Chronic thought suppression”. In: *Journal of Personality* 62 (1994), pp. 615–640. URL: <http://www.wjh.harvard.edu/~wegner/wbsi.html>.
- [84] F. Aoki et al. “Increased gamma-range activity in human sensorimotor cortex during performance of visuomotor tasks”. In: *Clinical Neurophysiology: Official Journal of the International Federation of Clinical Neurophysiology* 110.3 (Mar. 1999), pp. 524–537. ISSN: 1388-2457.
- [85] Pascal Fries et al. “Modulation of Oscillatory Neuronal Synchronization by Selective Visual Attention”. In: *Science* 291.5508 (Feb. 23, 2001), pp. 1560–1563. ISSN: 0036-8075, 1095-9203. DOI: 10.1126/science.1055465. URL: <http://science.sciencemag.org/content/291/5508/1560> (visited on 01/29/2019).
- [86] Kai J. Miller et al. “Spectral Changes in Cortical Surface Potentials during Motor Movement”. In: *Journal of Neuroscience* 27.9 (Feb. 28, 2007), pp. 2424–2432. ISSN: 0270-6474, 1529-2401. DOI: 10.1523/JNEUROSCI.3886-06.2007. URL: <http://www.jneurosci.org/content/27/9/2424> (visited on 01/29/2019).
- [87] Peter Brunner et al. “A Practical Procedure for Real-Time Functional Mapping of Eloquent Cortex Using Electrocorticographic Signals in Humans”. In: *Epilepsy & behavior : E&B* 15.3 (July 2009), pp. 278–286. ISSN: 1525-5050. DOI: 10.1016/j.yebeh.2009.04.001. URL: <https://www.ncbi.nlm.nih.gov/pmc/articles/PMC2754703/> (visited on 10/09/2018).
- [88] Jörn Rickert et al. “Encoding of Movement Direction in Different Frequency Ranges of Motor Cortical Local Field Potentials”. In: *Journal of Neuroscience* 25.39 (Sept. 28, 2005), pp. 8815–8824. ISSN: 0270-6474, 1529-2401. DOI: 10.1523/JNEUROSCI.0816-05.2005. URL: <http://www.jneurosci.org/content/25/39/8815> (visited on 01/29/2019).
- [89] Stephan Waldert et al. “Hand Movement Direction Decoded from MEG and EEG”. In: *Journal of Neuroscience* 28.4 (Jan. 23, 2008), pp. 1000–1008. ISSN: 0270-6474, 1529-2401. DOI: 10.1523/JNEUROSCI.5171-07.2008. URL: <http://www.jneurosci.org/content/28/4/1000> (visited on 01/29/2019).
- [90] Jae W. Chung et al. “Beta-band activity and connectivity in sensorimotor and parietal cortex are important for accurate motor performance”. In: *NeuroIm-*

- age 144 (Jan. 1, 2017), pp. 164–173. ISSN: 1053-8119. DOI: 10.1016/j.neuroimage.2016.10.008. URL: <http://www.sciencedirect.com/science/article/pii/S1053811916305559> (visited on 01/29/2019).
- [91] Tonio Ball et al. “Signal quality of simultaneously recorded invasive and non-invasive EEG”. In: *NeuroImage* 46.3 (July 1, 2009), pp. 708–716. ISSN: 1053-8119. DOI: 10.1016/j.neuroimage.2009.02.028. URL: <http://www.sciencedirect.com/science/article/pii/S1053811909001827> (visited on 08/16/2018).
- [92] Arne D. Ekstrom et al. “Human hippocampal theta activity during virtual navigation”. In: *Hippocampus* 15.7 (2005), pp. 881–889. ISSN: 1050-9631. DOI: 10.1002/hipo.20109.
- [93] Karim Jerbi et al. “Task-related gamma-band dynamics from an intracerebral perspective: Review and implications for surface EEG and MEG”. In: *Human Brain Mapping* 30.6 (June 1, 2009), pp. 1758–1771. ISSN: 1097-0193. DOI: 10.1002/hbm.20750. URL: <https://onlinelibrary.wiley.com/doi/abs/10.1002/hbm.20750> (visited on 10/05/2018).
- [94] Bradley C. Lega, Joshua Jacobs, and Michael Kahana. “Human hippocampal theta oscillations and the formation of episodic memories”. In: *Hippocampus* 22.4 (2012), pp. 748–761. ISSN: 1098-1063. DOI: 10.1002/hipo.20937. URL: <https://onlinelibrary.wiley.com/doi/abs/10.1002/hipo.20937> (visited on 01/30/2019).
- [95] C. D. Tesche and J. Karhu. “Theta oscillations index human hippocampal activation during a working memory task”. In: *Proceedings of the National Academy of Sciences* 97.2 (Jan. 18, 2000), pp. 919–924. ISSN: 0027-8424, 1091-6490. DOI: 10.1073/pnas.97.2.919. URL: <https://www.pnas.org/content/97/2/919> (visited on 01/30/2019).
- [96] Ole Jensen et al. “Oscillations in the Alpha Band (9–12 Hz) Increase with Memory Load during Retention in a Short-term Memory Task”. In: *Cerebral Cortex* 12.8 (Aug. 1, 2002), pp. 877–882. ISSN: 1047-3211. DOI: 10.1093/cercor/12.8.877. URL: <https://academic.oup.com/cercor/article/12/8/877/381083> (visited on 01/29/2019).
- [97] James F. Cavanagh and Michael J. Frank. “Frontal theta as a mechanism for cognitive control”. In: *Trends in Cognitive Sciences* 18.8 (Aug. 2014), pp. 414–421. ISSN: 13646613. DOI: 10.1016/j.tics.2014.04.012. URL: <https://linkinghub.elsevier.com/retrieve/pii/S1364661314001077> (visited on 01/30/2019).
- [98] R. E. Mistlberger, B. M. Bergmann, and A. Rechtschaffen. “Relationships among wake episode lengths, contiguous sleep episode lengths, and electroencephalographic delta waves in rats with suprachiasmatic nuclei lesions”. In: *Sleep* 10.1 (Feb. 1987), pp. 12–24. ISSN: 0161-8105.
- [99] S. Raghavachari et al. “Theta Oscillations in Human Cortex During a Working-Memory Task: Evidence for Local Generators”. In: *Journal of Neurophysiology* 95.3 (Mar. 1, 2006), pp. 1630–1638. ISSN: 0022-3077. DOI: 10.1152/jn.00409.2005. URL: <https://www.physiology.org/doi/full/10.1152/jn.00409.2005> (visited on 01/30/2019).
- [100] Philippe Kahane et al. “Invasive EEG in the definition of the seizure onset zone: depth electrodes”. In: *Handbook of Clinical Neurophysiology*. Vol. 3. Presurgical Assessment of the Epilepsies with Clinical Neurophysiology and Functional Imaging. Elsevier, Jan. 1, 2003, pp. 109–133. DOI: 10.1016/S1567-4231(03)03009-0. URL: <http://www.sciencedirect.com/science/article/pii/S1567423103030090> (visited on 10/12/2018).

- [101] Ingrid E. B. Tuxhorn, Reinhard Schulz, and Bernd Kruse. "Invasive EEG in the definition of the seizure onset zone: subdural electrodes". In: *Handbook of Clinical Neurophysiology*. Vol. 3. Presurgical Assessment of the Epilepsies with Clinical Neurophysiology and Functional Imaging. Elsevier, Jan. 1, 2003, pp. 97–108. DOI: 10.1016/S1567-4231(03)03008-9. URL: <http://www.sciencedirect.com/science/article/pii/S1567423103030089> (visited on 10/12/2018).
- [102] Adrian M. Siegel. "Presurgical evaluation and surgical treatment of medically refractory epilepsy". In: *Neurosurgical Review* 27.1 (Jan. 2004), 1–18, discussion 19–21. ISSN: 0344-5607. DOI: 10.1007/s10143-003-0305-6.
- [103] R. Cooper et al. "COMPARISON OF SUBCORTICAL, CORTICAL AND SCALP ACTIVITY USING CHRONICALLY INDWELLING ELECTRODES IN MAN". In: *Electroencephalography and Clinical Neurophysiology* 18 (Feb. 1965), pp. 217–228. ISSN: 0013-4694.
- [104] Dileep R. Nair et al. "Chronic subdural electrodes in the management of epilepsy". In: *Clinical Neurophysiology* 119.1 (Jan. 1, 2008), pp. 11–28. ISSN: 1388-2457. DOI: 10.1016/j.clinph.2007.09.117. URL: <http://www.sciencedirect.com/science/article/pii/S1388245707005810> (visited on 02/04/2019).
- [105] M.R. Sperling and M.J. O'Connor. "Comparison of depth and subdural electrodes in recording temporal lobe seizures". In: *Neurology* 39.11 (1989), pp. 1497–1504.
- [106] Michael Lang et al. "Advancements in Stereotactic Epilepsy Surgery: Stereoelectroencephalography, Laser Interstitial Thermotherapy, and Responsive Neurostimulation". In: *JHN Journal* 11.2 (2016). ISSN: 23252839. DOI: 10.29046/JHNJ.011.2.005. URL: <http://jdc.jefferson.edu/jhnj/vol11/iss2/5> (visited on 02/04/2019).
- [107] D. Zumsteg and H. G. Wieser. "Presurgical evaluation: current role of invasive EEG". In: *Epilepsia* 41 Suppl 3 (2000), S55–60. ISSN: 0013-9580.
- [108] H. Zhang and J. Jacobs. "Traveling theta waves in the human hippocampus". In: *Journal of Neuroscience* 35.36 (2015), pp. 12477–12487. DOI: 10.1523/JNEUROSCI.5102-14.2015.
- [109] I. Rektor et al. "Event-related potentials, cnv, readiness potential, and movement accompanying potential recorded from posterior thalamus in human subjects. A seeg study". In: *Neurophysiologie Clinique* 31.4 (2001), pp. 253–261. DOI: 10.1016/S0987-7053(01)00262-3.
- [110] M.R. Mercier et al. "Evaluation of cortical local field potential diffusion in stereotactic electro-encephalography recordings: A glimpse on white matter signal". In: *NeuroImage* 147 (2017), pp. 219–232. DOI: 10.1016/j.neuroimage.2016.08.037.
- [111] Rei Enatsu et al. "Combining stereoelectroencephalography and subdural electrodes in the diagnosis and treatment of medically intractable epilepsy". In: *Journal of Clinical Neuroscience: Official Journal of the Neurosurgical Society of Australasia* 21.8 (Aug. 2014), pp. 1441–1445. ISSN: 1532-2653. DOI: 10.1016/j.jocn.2013.12.014.
- [112] Jorge Gonzalez-Martinez et al. "Stereoelectroencephalography in the "difficult to localize" refractory focal epilepsy: early experience from a North American epilepsy center". In: *Epilepsia* 54.2 (Feb. 2013), pp. 323–330. ISSN: 1528-1167. DOI: 10.1111/j.1528-1167.2012.03672.x.
- [113] Stephan Chabardes et al. "Commentary: Understanding Stereoelectroencephalography: What's Next?" In: *Neurosurgery* 82.1 (Jan. 1, 2018), E15–E16. ISSN: 0148-396X. DOI: 10.1093/neuros/nyx499. URL: <https://academic.oup.com/neurosurgery/article/82/1/E15/4557100> (visited on 02/04/2019).

- [114] F. Cardinale et al. “Implantation of Stereoelectroencephalography Electrodes: A Systematic Review”. In: *Journal of Clinical Neurophysiology* 33.6 (2016), pp. 490–502. DOI: 10.1097/WNP.00000.00000000249.
- [115] D. H. Brainard. “The Psychophysics Toolbox”. In: *Spatial Vision* 10.4 (1997), pp. 433–436. ISSN: 0169-1015.
- [116] Suresh D. Muthukumaraswamy. “Functional Properties of Human Primary Motor Cortex Gamma Oscillations”. In: *Journal of Neurophysiology* 104.5 (Sept. 8, 2010), pp. 2873–2885. ISSN: 0022-3077. DOI: 10.1152/jn.00607.2010. URL: <https://www.physiology.org/doi/full/10.1152/jn.00607.2010> (visited on 02/05/2019).
- [117] Tetsuro Nagasawa et al. “Cortical gamma-oscillations modulated by auditory–motor tasks-intracranial recording in patients with epilepsy”. In: *Human Brain Mapping* 31.11 (2010), pp. 1627–1642. ISSN: 1097-0193. DOI: 10.1002/hbm.20963. URL: <https://onlinelibrary.wiley.com/doi/abs/10.1002/hbm.20963> (visited on 02/05/2019).
- [118] Victoria Southgate et al. “Predictive motor activation during action observation in human infants”. In: *Biology Letters* 5.6 (Dec. 23, 2009), pp. 769–772. DOI: 10.1098/rsbl.2009.0474. URL: <https://royalsocietypublishing.org/doi/full/10.1098/rsbl.2009.0474> (visited on 02/05/2019).